

## ABSTRACT

Title of Document: THEORETICAL AND EXPERIMENTAL  
EVALUATION OF ACETATE THRESHOLDS  
AS A MONITORING TOOL FOR IN SITU  
BIOREMEDIATION

Supida Piwkhaw, Master of Science, 2007

Directed By: Associate Professor, Eric A. Seagren  
Civil and Environmental Engineering  
Department  
Assistant Professor, Jennifer G. Becker  
Environmental Science and Technology  
Department

H<sub>2</sub> thresholds have been widely used to demonstrate the success of intrinsic bioremediation, however multiple problems exist in obtaining and interpreting H<sub>2</sub> field data. Acetate and H<sub>2</sub> play similar roles in the metabolism carried out by anaerobic microorganisms, and acetate thresholds have been observed in anaerobic subsurface environments. However, there is little understanding of the factors controlling acetate thresholds. This research used an integrated experimental study of pure cultures and environmental samples, along with microbial respiration modeling, to improve our understanding of acetate thresholds in various terminal electron accepting processes (TEAPs). The results demonstrated that acetate thresholds in pure cultures do not necessarily follow thermodynamic trends, as reported in previous studies, and the model evaluations under PCE-dechlorinating and Fe(III)-reducing

conditions revealed that kinetics play a greater role in controlling acetate thresholds in these TEAPs. Acetate thresholds measured in the environmental samples were influenced by the initial acetate concentrations. The results of this study improve our understanding of the factors influencing acetate thresholds in pure and mixed cultures and suggest that acetate thresholds may be a useful component of bioremediation monitoring programs.

THEORETICAL AND EXPERIMENTAL EVALUATION OF ACETATE  
THRESHOLDS AS A MONITORING TOOL FOR IN SITU BIOREMEDIATION

By

Supida Piwkhaw

Thesis submitted to the Faculty of the Graduate School of the  
University of Maryland, College Park, in partial fulfillment  
of the requirements for the degree of  
Master of Science  
2007

Advisory Committee:  
Dr. Eric A. Seagren, Chair  
Dr. Jennifer G. Becker, Chair  
Dr. Allen P. Davis

© Copyright by  
Supida Piwkhaw  
2007

## Acknowledgements

I must give my deepest appreciation to my advisors, Dr. Jennifer G. Becker and Dr. Eric A. Seagren, for their guidance, encouragement, and patience throughout the project. I also appreciate Dr. Allen P. Davis for devoting his time to serve as one of my committee members and for his advice on iron treatment method that was used in this study. Furthermore, I am thankful to Dr. Hubert Mantas for his help on my modeling work.

This project was initially funded by Maryland Water Resources Research Center. In addition to this fund, the project was also supported by the Environmental Science and Technology Department.

I am thankful to my lab mates, Deyang Huang, Yen-Jung Lai, Preston Postl, Gayle Davis, and Emily Deviller, for sharing their lab experiences with me and for making the lab enjoyable. I am especially thankful to Yen-Lung Lai for his company during the over-night sample collection and to Deyang Huang for his suggestion and help in the lab. I also appreciate Sheila Song for her partial work on the microcosm experiment.

I am especially grateful to my parents and sisters for sending their love and moral support continuously from Thailand in the past seven years. I am also thankful to my aunt and uncle in law, Supin and Ralph Horton, for their financial support throughout my higher educational career.

# Table of Contents

Acknowledgements.....	ii
Table of Contents.....	iii
List of Tables.....	iii
List of Figures.....	v
Chapter 1: Introduction.....	1
Chapter 2: Hypothesis, Objectives and Scope of Study.....	5
2.1 Hypothesis.....	5
2.2 Overall Goals and Objectives.....	6
2.3 Scope of Study.....	6
Chapter 3: Materials and Methods.....	8
3.1 Organisms and Media.....	8
3.2 Media Preparation and Culture Maintenance.....	13
3.3 Analytical Methods for the Pure Culture Experiments.....	16
3.3.1 <sup>14</sup> C-Labeled Acetate, Biomass, and Bicarbonate.....	16
3.3.2 Iron Analysis.....	20
3.3.3 Chlorinated Ethenes.....	22
3.3.4 Biomass.....	24
3.4 Mathematical Modeling.....	26
3.4.1 Model of Microbial Respiration.....	26
3.4.2 Estimation of $m$ and $\chi$ .....	30
3.5 Microcosm Experiment.....	32
3.5.1 Use of Microcosms to Evaluate Acetate Thresholds under Methanogenic Conditions.....	32
3.5.1.1 General Experimental Approach.....	32
3.5.1.2 Analytical Methods.....	34
Chapter 4: Background Information, Result, and Discussion.....	37
4.1 Background Information.....	37
4.2 Results and Discussion.....	43
4.2.1 Acetate Thresholds in Pure Culture Study.....	43
4.2.1.1 Results Obtained with <i>Geobacter metallireducens</i> .....	43
4.2.1.2 Results Obtained with <i>Desulfuromonas michiganensis</i> .....	45
4.2.1.3 Factor Influencing Acetate Thresholds.....	47
4.2.2 Result Obtained from Microcosm Study.....	61
Chapter 5: Conclusion and Recommendation for Future Work.....	66
References.....	69

## List of Tables

Table 3.1. Summary of cultures and conditions used in the various experiments.....	10
Table 3.2. Henry's constants of chlorinated ethenes at 30°C (Gossett, 1987).....	24
Table 3.3. Thermodynamic values of various chemical species used in current study.....	30
Table 4.1 Overall redox reactions for acetate oxidation coupled to the reduction of various electron acceptors, along with the associated standard free energy of reactions (Free energy calculated from the standard free energies of formation of the products and reactants by assuming standard conditions except for pH 7).....	39
Table 4.2 $S_{\min}^*$ values for various TEAPs (Seagren and Becker, 1999).....	42
Table 4.3. Summary of acetate thresholds, initial acetate concentrations, $\Delta G'_{30^\circ}$ and $\Delta G'_{30^\circ}$ in the batch threshold experiments.....	48
Table 4.4. Model parameter estimates fit to the experimental data.....	52
Table 4.5. Previously reported and current acetate threshold concentrations under various TEAPs .....	59
Table 4.6. Initial and threshold acetate concentrations in duplicate methanogenic sediment microcosms.....	63

## List of Figures

- Figure 4.1. Distribution of predominant TEAPs in sequential order away from contaminant source beginning with methanogenesis, sulfate reduction, Fe(III) reduction, nitrate and manganese reduction, and aerobic oxidation, respectively (Lovley, et al., 1994).....39
- Figure 4.2. Acetate depletion curves for strain GS-15 growing on 2.5 mM of acetate as the electron donor and (a) 50 mM Fe(III), (b) 25 mM Mn(IV), and (c) 6.25 mM  $\text{NO}_3^-$ . Each data point represents the average acetate concentration in triplicate batch reactors. Error bars represent  $\pm$  one standard deviation.....44
- Figure 4.3. Acetate depletion curves for strain BB1 growing on (a) 0.1 mM of acetate as the electron donor and 0.5 mM PCE, (b) 0.25 mM of acetate and 2.5 mM  $\text{S}^0$ , and (c) 0.5 mM of acetate and 10 mM Fe(III). Each data point represents the average acetate concentration in triplicate batch reactors. Error bars represent  $\pm$  one standard deviation.....46
- Figure 4.4. Acetate depletion data in triplicate or duplicate reactors of (a) strain GS-15 growing on Fe(III), and (b) strain BB1 growing on PCE under electron donor-limiting conditions. Data points represent individual experimental measurements. Lines represent the best fit of Equation 4.3 to the pooled experimental data.....51
- Figure 4.5. Reduced species accumulation data in triplicate reactors of (a) strain GS-15 growing on Fe(III), and (b) strain BB1 growing on PCE with excess acetate. Data points represent individual experimental measurements. Lines represent the best fit of Equation 3.5 to the pooled experimental data.....52
- Figure 4.6. Comparison of experimental data and model predictions for strain GS-15 growing under dual substrate-limiting conditions: (a) acetate (2.5 mM) and (b) Fe(II) (from 20 mM Fe(III)). Each data point represents an individual measurement. Lines represent model predictions using  $K'_D$  and  $K_A$  values estimated at 2.5 mM acetate (Table 4.3).....54
- Figure 4.7. Comparison of experimental data and model predictions for strain BB1 growing under dual substrate-limiting conditions: (a) acetate (0.25 mM) and (b) aqueous concentration of daughter products of PCE (*cis*DCE and TEC). Each data point represents an individual measurement. Lines represent model predictions using  $K'_D$  and  $K_A$  values estimated at 0.1 mM and 0.25 mM acetate, respectively (Table 4.3).....54



Figure 4.8: Evaluation of  $F_T$ ,  $F_D$ ,  $F_A$ , and  $v$ ; Strain GS-15 growing on Fe(III) using 2.5 mM acetate (a) and 0.5 mM (b) of acetate; and (c) Strain BB1 grown under limiting acetate using PCE as electron acceptor. The  $F_T$  values calculated for strain GS-15 were based on assumed concentrations of Fe(III) and Fe(II) because these values were not measured during the threshold experiments.....56

Figure 4.9 Acetate concentrations and cumulative methane production in duplicate microcosms spiked repeatedly with acetate (on days 24, 46, 79, 128, 166, 208, 312, and 390). Sulfate (2 mM) was also added on days 208, 312, and 390. The methanogenic inhibitor BES (2 mM) was also added on days 312 and 390 to promote sulfate reduction. ↓ indicates the first time when sulfate was amended to the reactor.....62

Figure 4.10. Acetate thresholds as a function of initial acetate concentrations in duplicate sediment microcosms under methanogenic and sulfate-reducing condition. Each data point represents the average concentrations in duplicate microcosms..65

# Chapter 1

## Introduction

Industrial development and population growth have contributed to groundwater contamination throughout the United States. Major sources of groundwater contamination, particularly volatile organic compounds (VOCs), come from leakage of gasoline storage tanks and sewer systems, storm water runoff, lawn irrigation, and wide spread use of chemicals in commercial and residential areas (Squillace et al., 2004). Unfortunately, the presence of chemical contaminants in groundwater can prohibit the use of this valuable resource for drinking water and other applications. According to Hutson et al. (2005), over 70% of the water supply in the United States comes from groundwater, so a deterioration in the quality of this water resource could significantly impact the well being of the population as a whole.

Fortunately, many common groundwater contaminants can be degraded by native bacteria. In some cases, the bacteria can use different contaminants as an electron donor (e.g., petroleum hydrocarbons) or electron acceptor (e.g., polychlorinated ethenes) to generate free energy for growth and/or maintenance. The result is the destruction and/or transformation of these compounds. Bioremediation is a remedial approach that takes advantage of these biological processes to clean up chemically contaminated sludge, soil, or groundwater (Cookson, 1995).

Several bioremediation approaches have been developed to cleanup groundwater contamination including engineered *ex-situ* bioremediation, engineered *in-situ*

bioremediation, and intrinsic *in-situ* bioremediation (otherwise known as monitored natural attenuation). The approaches are distinguished from one another by the location of the treatment and the aggressiveness of the treatment. When contaminated groundwater is pumped out and the treatment occurs above ground it is often referred to as an *ex-situ* treatment, whereas if the groundwater is remediated in place it is referred to as *in-situ* treatment. Engineered bioremediation is accomplished by enhancing the rate of biodegradation through the use of intrusive engineering applications (e.g., addition of substrates, nutrients, etc.), while intrinsic bioremediation is done by allowing the indigenous microbial consortia to degrade the contaminants at their natural rate under the existing condition (NRC, 2000).

*In situ* bioremediation has several advantages over *ex-situ* clean up technologies, such as pump and treat, because it generally requires lower capital costs, and the clean up can be done on site thus reducing the liability that may occur during waste transportation (Cookson, 1995). However, *in-situ* bioremediation is often still thought of as an unproven technology, given that its success can not be guaranteed due to the lack of technical knowledge of the subsurface's dynamics and relatively limited experience with this technology in the field (Cookson,1995). This is particularly true with natural attenuation, in which case laboratory studies and field-scale pilot studies cannot always accurately predict field results and the possibility exists that the plume can bypass sampling stations and be missed by monitoring efforts (NRC, 2000).

To overcome these problems, the NRC (2000) committee on *in situ* bioremediation proposed that two lines of evidences are required for indication of successful *in-situ* bioremediation. First, there should be sound scientific evidence illustrating that the proposed removal mechanisms are possible for the site setting. Second, there needs to be cause and effect evidence showing that the proposed removal mechanisms are actually taking place at the real site. While the first type of evidence can be relatively easily obtained, the second type of evidence is often difficult to demonstrate. In general, multiple indicators, or lines of evidence are needed to prove that the depletion or attenuation of contaminants has occurred as a result of microbial activities. These indicators are often obtained from microbial "footprints", a term that refers to a variety of indicators of the activity of contaminant-degrading microorganisms. Thus microbial footprints may include increases in the concentrations of metabolic byproducts (e.g., reduced electron acceptor species), evidence of substrate consumption (e.g., a decrease in electron donor concentrations), and pH changes due to contaminant transformation (NRC, 2000) to name a few. Of particular relevance to this study, H<sub>2</sub> thresholds are sometimes used in *in situ* bioremediation to evaluate whether terminal electron acceptors are being depleted. As discuss in greater detail in Chapter 4, if the contaminant of interest serves as an electron donor to microorganisms, its metabolism will deplete terminal electron acceptors. In theory, the most energetically-favorable electron acceptors will be depleted first, followed in succession by less favorable electron acceptors. Characteristic H<sub>2</sub> thresholds are thought to exist for different terminal electron accepting processes (TEAPs). Thus, *in situ* H<sub>2</sub> levels should increase as

biodegradation of contaminants proceeds. Because acetate and H<sub>2</sub> play similar roles in anaerobic metabolic pathways, it seems reasonable that acetate might also be related to the dominant TEAP.

However, Seagren and Becker (2002) note that measurement of these footprint parameters using the currently available technologies is challenging, and quantitative interpretation of these data in natural settings is often ambiguous. Having more easily obtained indicators to prove that clean up goals are being accomplished as a result of microbial activity will help promote the widespread use of *in situ* bioremediation. Therefore, the overall goals of this research were to improve our understanding of the fundamental factors controlling acetate thresholds, evaluate whether a relationship exists between the dominant terminal electron accepting process (TEAP) and acetate thresholds, and evaluate whether acetate thresholds can be used as a practical monitoring tool for successful *in-situ* bioremediation of a contaminated site.

The following chapters concisely describe this research. First, Chapter 2 provides the hypothesis, objectives, and scope of the study. The experimental materials and methods used in this research are subsequently described in detail in Chapter 3. Chapter 4 is a draft manuscript (minus the materials and methods section) and provides a brief review of the background information necessary to understand this research as well as the key experimental results and discussion. Finally, Chapter 5 presents a summary and conclusions of this work, along with recommendations for future research.

## Chapter 2

### Hypothesis, Objectives and Scope of Study

#### 2.1 Hypothesis

As mentioned in the previous Chapter, minimum or threshold  $H_2$  concentrations have been shown to exist under anaerobic conditions and appear to be characteristic of the dominant terminal electron accepting process (TEAP) (Lovley and Phillips, 1988b). Therefore, it has been proposed that  $H_2$  can be used as an indicator of the predominant TEAP (e.g., in subsurface systems undergoing *in situ* bioremediation). Acetate thresholds have also been observed under anaerobic conditions, though they have not been studied to the same extent as  $H_2$  thresholds. Acetate and  $H_2$  play similar roles as intermediates in the biodegradation pathways of organic compounds under anaerobic conditions. Therefore, it is hypothesized that different characteristic threshold acetate concentrations occur in regions of a plume that are dominated by different TEAPs and could be a useful component of bioremediation monitoring programs. Specifically, if the magnitude of the acetate thresholds changes due to a shift in the dominant TEAP, it could provide evidence that a contaminant is being utilized by microorganisms as an electron donor. However, in order to correctly interpret changes in acetate thresholds, an understanding of how acetate thresholds are related to the dominant TEAP and the factors that control acetate thresholds is needed.

## **2.2 Overall Goals and Objectives**

The overall goal of this research is to improve our understanding of the relationship between the dominant TEAP and acetate thresholds and evaluate the usefulness of acetate thresholds as an indicator of biodegradation in contaminated subsurface environment. To achieve this goal and to evaluate the above hypothesis, an integrated experimental and modeling study was designed with the following specific objectives:

- 1) measure the acetate thresholds in two pure cultures growing on limiting amounts of acetate under a variety of anaerobic TEAPs;
- 2) fit the parameters of a respiration model to experimental measurements of acetate oxidation and electron acceptor reduction under two different sets of conditions;
- 3) determine whether thermodynamic and/or kinetic factors control acetate thresholds for each TEAP using the mathematical model;
- 4) evaluate the usefulness of acetate thresholds as an indicator of dominant TEAPs in contaminated subsurfaces; and
- 5) measure the acetate thresholds under different TEAPs in microcosms containing sediment and groundwater collected from a contaminated site.

## **2.3 Scope of Study**

Overall this research systematically examined the research hypothesis by quantifying acetate threshold concentrations under highly defined and controlled experimental conditions. The data obtained from these proof-of-concept experiments were then compared with an existing mathematical model of microbial respiration to determine

whether kinetic and/or thermodynamic factors control the acetate threshold concentration for each TEAP. The microcosm study was conducted to evaluate the hypothesis under environmental conditions.

More specifically, this study investigated the characteristic acetate threshold concentrations under Fe(III)-, Mn(IV)-, and NO<sub>3</sub><sup>-</sup>-, PCE-, and S<sup>0</sup>-reducing conditions using two anaerobic microorganisms, *Desulfuromonas michiganensis* (strain BB1) and *Geobacter metallireducens* (strain GS-15). In this thesis, the two cultures will be referred to as strain GS-15 and strain BB1, respectively. Strain GS-15 was used in experiments conducted under three different TEAPs including Fe(III)-, Mn(IV)-, and NO<sub>3</sub><sup>-</sup>-reducing conditions, while strain BB1 was used in experiments under Fe(III)-, tetrachloroethene (PCE)-, and S<sup>0</sup>-reducing conditions. The microcosm study investigated characteristic thresholds under methanogenic and sulfate-reducing conditions. These TEAPs were selected because they are often observed at sites contaminated with hydrocarbons. The pure cultures were selected based on their abilities to utilize the electron acceptors of interest.



## Chapter 3

### Materials and Methods

This chapter provides a detailed description of the materials and analytical methods used for the threshold experiments as well as the mathematical respiration model and the methods used to estimate the model parameters. First, the media components used for culturing different microbial species are described. Second, the general culture techniques used for preparing the cultures and the procedures for performing threshold experiments are explained. Third, the analytical methods are described. Fourth, the procedures used to fit the model to the threshold experiment data are explained. Last, the experimental procedures for the microcosm studies are briefly described.

#### 3.1 Organisms and Media

Both strain GS-15 (DSM No. 7210) and strain BB1 (DSM No. 15941) were obtained from the German Collection of Microorganisms and Cell Cultures (DSMZ) (DSMZ Versand, Braunschweig, Germany). A total of five sets of experiments were conducted with each of the strains used in this research (strain GS-15 and strain BB1). For each organism, three of these experiments were designed so that key parameters in the respiration model could be fit to the data. In these experiments, the concentrations of the oxidized and reduced forms of the electron donor (acetate),  $[D^+]$  and  $[D^-]$ , respectively, were monitored over time along with the concentrations of the oxidized and reduced forms of the electron acceptor,  $[A^+]$  and  $[A^-]$ , respectively.

These parameter-fitting experiments were conducted for strain GS-15 growing on Fe(III) under electron acceptor-limiting, electron donor-limiting, and dual substrate-limiting conditions. Similarly, model parameters were fit to data obtained with strain BB1 grown via PCE dechlorination under electron acceptor-limiting, electron donor-limiting, and dual substrate-limiting conditions. The experiments done with strain GS-15 growing on Fe(III) and strain BB1 growing on PCE under electron donor-limiting conditions also yielded acetate threshold data. In addition, strain GS-15 was grown on limiting amounts of acetate under Mn(IV)- and NO<sub>3</sub><sup>-</sup>-reducing conditions and strain BB1 was grown on limiting amounts of acetate under Fe(III)- and S<sup>0</sup>-reducing conditions to obtain acetate thresholds under different TEAPs. In these experiments, only acetate concentrations were measured. A summary of the experiments conducted, including the cultures, corresponding TEAPs, substrate concentrations, and the ratio between the electron donor and acceptor, is provided in Table 3.1.

The basal medium used for culturing strain GS-15 (Lovley and Philips, 1988) contained the following constituents (per liter of media): NaHCO<sub>3</sub>, 2.5 g; NH<sub>4</sub>Cl, 0.25 g; KCl, 0.1 g; NaCH<sub>3</sub>COOx3H<sub>2</sub>O (Fisher-Scientific, 99.8%), 0.34 g (except for the experiment under Fe(III)-limiting conditions in which 2.72 g was used), and 10 ml of Wolfe's trace mineral solution (Ferguson and Mah, 1983). Strain GS-15 was also provided with the electron acceptor needed to establish the appropriate TEAP. For the iron-reducing experiments, ferric citrate (FeC<sub>6</sub>H<sub>5</sub>O<sub>7</sub>, Sigma-Aldrich, 16.5-18.5%

Table 3.1. Summary of cultures and conditions used in the various experiments.

Culture	Terminal electron acceptor	Limiting substrate	e- donor concentration (mM)	e- acceptor concentration (mM)	Ratio of e- donor to e- acceptor <sup>a</sup>
<i>Geobacter metallireducens</i> strain GS-15	Fe(III)	e- acceptor	20	40	4:1
		dual substrate	2.5	20	1:1
		e- donor	2.5	50	1:2.5
	Mn(IV)	e- donor	0.5	10	1:2.5
		e- donor	2.5	25	1:2.5
		e- donor	2.5	6.25	1:2.5
<i>Desulfuromonas michiganensis</i> strain BB1	PCE	e- acceptor	0.25	0.05	2.5:1
		dual substrate	0.25	0.5	1:1
		e- donor	0.1	0.5	1:2.5
	S <sup>0</sup>	e- donor	0.25	2.5	1:2.5
	Fe(III)	e- donor	0.5	10	1:2.5

<sup>a</sup> Ratios calculated on an electron equivalence basis. The following electron equivalences were used in calculating the ratios: acetate/CO<sub>2</sub>, 8 e<sup>-</sup> eq; Fe(II)/Fe(III), 1 e<sup>-</sup> eq; Mn(II)/Mn(IV), 2 e<sup>-</sup> eq; NH<sub>4</sub><sup>+</sup>/NO<sub>3</sub><sup>-</sup>, 1 e<sup>-</sup> eq; cisDCE/PCE, 2 e<sup>-</sup> eq; and HS<sup>-</sup>/S<sup>0</sup>; 2 e<sup>-</sup> eq.

iron), was added to the media at three different concentrations: 9.78 g/L, 12.23 g/L, and 4.89 g/L, under Fe(III)-limiting, dual substrate-limiting, and acetate-limiting conditions, respectively. For the experiment conducted under nitrate respiring conditions, NaNO<sub>3</sub> (Fisher-Scientific, 99%), (0.53 g/L) was added to the media in place of ferric citrate. 0.1 ml of cysteine solution (17.5g cysteine-HCl x H<sub>2</sub>O/100 ml) was also added to the nitrate reducing media as a reducing agent and to prevent cell lysis (Lovley, personal communication 2007), and 50 μM of ferric iron was added because iron is required during nitrate respiration (Senko and Stolz, 2001). For the Mn(IV)-reducing experiment, ferric citrate was replaced with 250 ml of a solution of poorly crystallized MnO<sub>2</sub> (100 mM). MnO<sub>2</sub> was prepared from KMnO<sub>4</sub> (J. T. Baker, 99.6%), NaOH (Fisher-Scientific, 98.1%), and MnCl<sub>4</sub>x4H<sub>2</sub>O (Fisher-Scientific, 98–101 %) as described by Lovley and Philips (1988a).

Strain GS-15 is typically grown on 20 mM acetate (Lovley and Philips, 1988a), and this concentration was used in the experiment conducted under electron acceptor-limited conditions (Table 3.1). However, in order for 20 mM acetate to be limiting, the Fe(III) concentration had to be increased to 400 mM, which inhibited the growth of strain GS-15. Therefore, in the remaining experiments involving strain GS-15, a lower acetate concentration of 2.5 mM was used for experiments conducted under electron donor-limiting or dual substrate-limiting conditions to eliminate concerns about Fe(III) toxicity. The constant acetate concentration also prevented any variation in the threshold concentrations due to the use of different initial substrate concentrations. This acetate concentration resulted in ratios between the electron donor and acceptor ranging from 1:1 to 1:2.5 on an e- equivalence basis (Table 3.1).

Strain BB1 was grown on the low chloride (LC) basal medium described by Sung et al. (2003). The media contained the following constituents (per liter of media):  $\text{MgSO}_4 \cdot 7\text{H}_2\text{O}$ , 0.54 g;  $\text{NH}_4\text{SO}_4$ , 0.3 g;  $\text{K}_2\text{SO}_4$ , 0.3 g;  $\text{CaSO}_4 \cdot 2\text{H}_2\text{O}$ , 0.017g;  $\text{KH}_2\text{PO}_4$ , 0.2 g;  $\text{NaHCO}_3$ , 2.5 g; and 1 ml each of trace element solutions A and B, which have been described by Löffler et al. (1996). In addition, the basal media was amended with an appropriate electron acceptor. For the PCE dechlorination experiment, neat PCE was added to the media bottle to yield a final concentration of 0.05 mM under the PCE-limiting condition and 0.5 mM under both dual substrate-limiting and acetate limiting conditions. For the  $\text{S}^0$ -reducing experiment,  $\text{S}^0$  powder was suspended in deoxygenated DDI water (80 g/L), and pasteurized at 90°C for 15 minutes. Then the suspended  $\text{S}^0$  was anaerobically transferred to the media bottle to yield a final concentration of 2.5 mM. 2.5 mM of Fe(II) was also added to the  $\text{S}^0$  media from a stock  $\text{FeCl}_2 \cdot 7\text{H}_2\text{O}$  solution (28 g/L) to precipitate and reduce the toxicity of the sulfide produced by sulfur reduction. For the experiment conducted under iron-reducing conditions, Fe(III) was added to the media from a stock ferric citrate solution (122.3 g/L) to yield a final concentration of 10 mM. The stock iron solution was neutralized to pH 7 with 10 N NaOH.

These new experimental conditions resulted in electron donor/electron acceptor ratios of 1:1 to 1:2.5, as for strain GS-15. However, because PCE exhibits toxicity to strain BB1 at 0.5 mM (Huang, personal communication 2007) and strain BB1 could not grow at iron concentration exceeding 10 mM (based on preliminary investigations) a constant acetate concentration could not be used for all experiments. Therefore, to avoid electron acceptor toxicity in the PCE dechlorination and iron reducing

experiments and ensure that the correct substrate was limiting, acetate concentrations ranging from 0.1 to 0.5 mM were used for the experiments involving strain BB1 (Table 3.1).

### **3.2 Media Preparation and Culture Maintenance**

All media preparations, additions, transfers, and inoculations were performed using an anaerobic gassing manifold system. The syringes used for all culture transfers and additions were first purged with anoxic gas to remove oxygen. Glassware used for the experiments was cleaned with phosphate-free detergent (Alconox), triple rinsed with DDI water, allowed to air dry, and baked at 380°C for 3 hours.

The basal media described above was prepared by adding all the constituents to approximately 1 L of DDI water that had been boiled and cooled to room temperature under an N<sub>2</sub>/CO<sub>2</sub> atmosphere (80:20, v/v, AirGas East). An exception was made to this procedure when adding ferric citrate. To increase its solubility in DDI water, ferric citrate was added when the water was still near its boiling temperature. The solution was then cooled down to room temperature, and the pH was adjusted to 6 with 10 N NaOH before the other constituents were added. After the media was mixed thoroughly, the pH was adjusted, if necessary, to reach a final value of 7, 100 ml-aliquots were anaerobically transferred to deoxygenated 160-ml serum bottles, which were sealed with thick black butyl rubber septa (Geo-Microbial Technologies, Inc.) and aluminum crimp caps. These serum bottles are hereafter referred to as batch reactors. The batch reactors were autoclaved at 121°C for 20 minutes and were cooled down to room temperature. Each batch reactor used in a strain GS-15

experiment was then amended with 1 ml each of stock  $\text{NaH}_2\text{PO}_4 \cdot \text{H}_2\text{O}$  buffer solution (6 g/L) and Wolfe's vitamin solution (Ferguson and Mah, 1983) using sterile needles and syringes. Using the same procedure, each batch reactor used in a strain BB1 experiment was also amended with 1 ml of Wolfe's vitamin solution, 0.25 ml of  $\text{Na}_2\text{S} \cdot 9\text{H}_2\text{O}$  stock solution (20 g/L) as a reducing agent, and 1 ml of resazurin solution (0.1 g/L) as a redox indicator. If acetate was not included in the basal media, it was added to the batch reactor from a sterile stock solution prior to inoculation. This method of acetate addition was always used for strain BB1 and for batch experiments involving strain GS-15.

The stock acetate, cysteine, sodium phosphate buffer, sodium sulfide and resazurin solutions were anaerobically prepared, autoclaved, and stored at 4°C. Wolfe's vitamin solution was filter-sterilized (0.2  $\mu\text{m}$ ) and transferred to serum bottle that was deoxygenated, sealed with a black rubber septum and crimp cap, and stored under 4°C.

Before being used for the experiments, strain GS-15 was revived from lyophilized pellets and transferred at least 10 times. Strain BB1 was provided by Deyang Huang of the Environmental Science and Technology Department at the University of Maryland, College Park. The media routinely used to maintain strain GS-15 contained 20 mM acetate and 40 mM of ferric iron, while that used for maintenance of strain BB1 contained 0.25 mM acetate and 0.5 mM of PCE. Both strains were incubated statically in the dark at 30°C with one exception. Strain BB1 was continuously shaken (120 rpm) when grown on PCE.

Before being used as the inoculum for a batch reactor, strain GS-15 was allowed to completely reduce ferric iron in the media, and the biomass was then harvested by centrifugation and resuspended in the appropriate medium. The volume of the inoculum varied so that the initial ratio of the limiting substrate concentration to the biomass concentration ( $S_0:X_0$ ) was greater than 20:1 when both  $S_0$  and  $X_0$  were expressed on a chemical oxygen demand (COD) basis. By providing a large amount of substrate to a small amount of biomass, the cells in the batch assays should have been able to grow unrestricted, and therefore, the parameter estimates should have been independent of the culture's history (Grady et al., 1996). For strain BB1, the source culture was allowed to completely utilize acetate and remove PCE. When harvesting strain BB1 biomass, the culture medium was first purged with  $N_2$  (Ultra high purity grade, AirGas East) for 15 minutes and then purged with  $N_2/CO_2$  (80:20, v/v) for 5 minutes to strip off volatile chlorinated daughter products of PCE dechlorination and equilibrate  $CO_2$  in the headspace with  $HCO_3^-$  in the medium, respectively. The volume of culture needed to yield  $S_0:X_0$  greater than 20:1 was then transferred to each batch reactor. At least 3 hours prior to an experiment, a mixture of  $^{14}C$ -labeled and un-labeled acetate (discussed in the following section) was added to the batch reactors used for experiments under electron donor- and dual substrate-limiting conditions, while the batch reactors used for experiments under electron acceptor-limiting conditions received only unlabeled acetate.

A single control was also prepared for each experiment in the same way as the batch reactor. The controls were amended with unlabeled acetate only, as well as inoculum, with the exception of the experiments involving strain BB1 growing on PCE, which



were not inoculated. Immediately after being inoculated, controls were autoclaved at 120°C for 20 minutes to inactivate the cells, so that any abiotic removal of acetate could be measured.

### **3.3 Analytical Methods for the Pure Culture Experiments**

#### **3.3.1 <sup>14</sup>C-Labeled Acetate, Biomass and Bicarbonate**

Conventional chromatographic approaches such as gas chromatography (GC), high performance liquid chromatography, and ion chromatography cannot be used to quantify acetate in the nM range. Acetate thresholds were anticipated to be in the nM range based on the magnitude of H<sub>2</sub> thresholds measured under anaerobic conditions (e.g., Cord-Ruwisch et al., 1988; Löffler et al., 1999). Therefore, acetate was measured using a radiolabeling approach like that described by He and Sanford (2004) and Freedman (1991). Specifically, a mixture containing known amounts of [1,2-<sup>14</sup>C]CH<sub>3</sub>COONa ([<sup>14</sup>C]acetate) and un-labeled acetate solution was added to batch reactors operated under electron donor- or dual substrate-limiting conditions at least one hour prior to the beginning of experiment. [<sup>14</sup>C]acetate (50 μCi) was obtained from Moravek (≥ 96% purity, specific activity 100-120 μCi/μmol) and aseptically diluted in 10 ml of sterile DDI water, and stored at -4°C until needed in an experiment. [<sup>14</sup>C]acetate was quantified using liquid scintillation counting, following high performance liquid chromatography (HPLC) separation of acetate from other sample constituents. The un-labeled acetate was then quantified using the ratio of [<sup>14</sup>C]acetate to un-labeled acetate in the stock solution.

The advantage of using the radiolabeling method to determine acetate thresholds is that it could also be used to quantify biomass (X) and bicarbonate plus carbon dioxide ( $D^+$ ). To measure [ $^{14}C$ ] activity in the acetate, biomass, and  $HCO_3^-/CO_2$  fractions, liquid samples were regularly withdrawn from the batch reactors. At each sampling event, a total of 1.7 ml was removed from each batch reactor and split into four subsamples. The subsamples were treated as follows: (1) 0.2 ml was transferred to a 7-ml liquid scintillation vial containing 5 ml of LSC. (2) 1 ml was filtered into a 1-ml HPLC sample vial (Waters Inc.) using a 0.2  $\mu m$  syringe filter (Millex-LG, 4 mm diameter, Fisher Scientific) and 0.2 ml of this filtrate was added to 5 ml of LSC. (3) 0.25 ml of the subsample 2 filtrate was analyzed by HPLC, as described below. This sample was referred to as subsample 3. (4) The remaining 0.5 ml sample of culture was used for bicarbonate quantification. Initially the following approach was used. The 0.5 ml sample was incubated with 0.1 ml barium chloride (350 mM) for 10 minutes to precipitate out  $BaCO_3$ . The mixture was then centrifuged for 10 minutes at 13,000 rpm in a microcentrifuge (Eppendorf, model 5415C) before being filtered with a 0.2  $\mu m$  membrane syringe filter (Millex-LG, 4 mm diameter). The filtrate (0.2 ml) (referred to as subsample 4) was transferred to a scintillation vial containing 5 ml of LSC and counted.

The activity in subsample 1 represents the total  $^{14}C$  activity in a culture ( $[^{14}C]_{acetate} + [^{14}C]_{biomass} + [^{14}C]_{HCO_3^-}$ ).  $[^{14}C]_{biomass}$  was calculated by subtracting the activity in subsample 2 from subsample 1. The activity in subsample 3 represents  $[^{14}C]_{acetate}$ . It was thought subtracting the activity in subsample 4 from subsample 1 would give an estimate of  $[^{14}C]_{HCO_3^-}$ . However a problem was detected with this

approach. The activity measured in subsample 4 was too high due to interference caused by cloudy characteristics of the sample. In fact, the activity recovered in subsample 4 was often much higher than in subsample 3, which also should have contained only the [ $^{14}\text{C}$ ]acetate. Because of this problem, the [ $^{14}\text{C}$ ]bicarbonate concentration was calculated by subtracting subsample 3 from subsample 2.

A different approach was adopted for bicarbonate quantification in the Fe(III)-reducing experiments using strain GS-15 and strain BB1 growing on 0.5 mM of acetate and involved removal of  $\text{HCO}_3^-/\text{CO}_2$  from the samples. When using this procedure, 1 ml of sample was removed from a batch reactor and filtered as previously described. The filtrate was acidified with 0.1 N HCl to lower pH to the range of 4.5 and 6, and then sparged with  $\text{N}_2$  (100%) for 10 minutes to drive off  $\text{CO}_2$ . The remaining sample, which presumably contained only acetate, was transferred to a 1-ml HPLC vial and analyzed with the HPLC. The [ $^{14}\text{C}$ ]bicarbonate concentration was calculated by subtracting the activity in this subsample from the  $^{14}\text{C}$  activity in subsample 2. This approach not only allowed quantification of bicarbonate species but also prevented  $\text{HCO}_3^-$  from co-eluting with acetate as discussed further below.

Quantification of  $\text{CO}_2$  in the gas phase at the conclusion of the batch threshold experiments was also attempted in this research. A headspace sample (4 ml) was collected using a gas-tight syringe and transferred to a liquid scintillation vial containing 1 ml of Carbosorb E, a  $\text{CO}_2$ -trapping reagent (PerkinElmer), and 5 ml of Permaflur E+ LSC (PerkinElmer). However, the activities measured using this method varied greatly from sample to sample, therefore, this method of measuring

CO<sub>2</sub> (g) was discontinued and instead, CO<sub>2</sub> (g) was calculated using its equilibrium constant with bicarbonate and Henry's constant.

A Waters Carbamate HPLC equipped with a model 717 plus pump, and model 600 controller, and a RSpak KC-811 column (8.0 mm ID x 300 mm, Shodex) maintained at 50°C in a Waters temperature control module was used to separate [<sup>14</sup>C]acetate from other sample constituents in subsample 3. A flow rate of 1 ml/min was used with phosphoric acid in DDI water (pH 2, 0.1 % v/v) as the mobile phase. The effluent from a Waters Model 996 photodiode array detector was routed to a fraction collector (Model III; Waters, Inc.). To determine the fraction corresponding to acetate, 250 µL of 1600 mM unlabelled acetate was injected on to the HPLC, and 0.5 minute fractions were collected. The fractions were reinjected and the relative amount of unlabeled acetate in each fraction was determined by monitoring peak area using the photodiode array detector. At the time when the effluent collection interval was first determined, 117% of the acetate could be recovered by collecting the effluent from 10 to 12 min after the sample was injected. This collection interval was used for all experiments involving strain GS-15. Over time, the elution time of acetate broadened due to a degradation of the ion exchange column caused by loading with high concentrations of carbonate species. Therefore, the effluent collection time was reevaluated using the above procedure. For the experiments involving strain BB1, the effluent was collected from 10 to 14 min.

It was subsequently determined that the longer effluent collection interval used for strain GS-15 partially overlapped with bicarbonate eluting from the HPLC system.

The presence of bicarbonate in acetate fraction was confirmed by injecting 250  $\mu\text{l}$  of 500  $\mu\text{M}$  [ $^{14}\text{C}$ ] $\text{HCO}_3\text{Na}$  labeled bicarbonate (Moravek, Inc., purity  $\geq 97\%$ ; specific activity 50-60  $\mu\text{Ci}/\mu\text{mol}$ ) onto the HPLC, collecting the effluent in 1 minute intervals, and counting the samples in 5 ml of LSC. Bicarbonate began eluting at 12.5 minutes; therefore, the 10 – 14 minute collection interval used to trap acetate in the strain BB1 experiments also captured some bicarbonate. Because of this problem, the samples collected under electron donor-limiting conditions when strain BB1 was growing on PCE were reanalyzed using 2 minute collection interval. The acetate concentrations measured under electron donor-limiting conditions when strain BB1 was growing on  $\text{S}^0$  were multiplied by a correction factor that takes into account the fraction of the  $^{14}\text{C}$  activity measured in 10 – 14 minute trapping interval that was due to [ $^{14}\text{C}$ ] acetate.

All samples containing radioactivity were counted for 10 minutes in a liquid scintillation counter (Packard, model 1600CA-Tri-Carb). An internal standard quench curve was used to correct for the counting efficiency, which was then used for calculation of the specific activity. Ecoscint XR liquid scintillation cocktail (LSC, National Diagnostic, Inc.) was used for counting all samples.

### **3.3.2 Iron**

Total Fe,  $\text{Fe}^{3+}$ , and  $\text{Fe}^{2+}$  were analyzed using a modification of the bipyridine method developed by the U.S. Geological Survey (Brown et al., 1970). It should be noted that while total Fe and  $\text{Fe}^{2+}$  can be directly measured, quantification of  $\text{Fe}^{3+}$  can only be obtained by subtracting  $\text{Fe}^{2+}$  from the total Fe concentration. A 1-ml aliquot of sample was withdrawn from the reactor using a sterile needle and syringe and

transferred to a centrifuge tube (15 ml) for analysis of Fe species. The sample was immediately treated with concentrated nitric acid (15-16 N) to lower the pH to 2-3 and then capped. This step was done to prevent oxidization of  $\text{Fe}^{2+}$ . Samples were stored at 4°C until the Fe analysis could be performed.

For  $\text{Fe}^{2+}$  analysis, a stock solution was prepared by dissolving  $\text{Fe}(\text{NH}_4)_2(\text{SO}_4)_2 \times 6\text{H}_2\text{O}$  in DDI water (1.4 g/L). Five concentrations of  $\text{Fe}^{2+}$  standards (0, 10, 40, 80, and 100 mg/L) were prepared in 10-ml volumetric flasks by diluting the stock solution with DDI water. 0.5 ml of bipyridine solution (2 g 2,2-bipyridyl/L) was then added. Next the standard was mixed by hand, capped, and allowed to react for 30 minutes. The standard was then amended with 1 ml of 580 g  $\text{CH}_3\text{COONa} \times 3\text{H}_2\text{O}/\text{L}$  and mixed thoroughly. The absorbance of the standards was measured at 520 nm using a spectrophotometer (Bausch & Lomb, Spectronic 20). The  $\text{Fe}^{2+}$  concentration in the samples was determined by comparison with the external standards.

A similar approach was used for total Fe analysis. A stock solution was prepared by dissolving 0.1 g of clean iron wire (99.99%, 0.01 in diameter, Puratronic) in 10 ml of approximately 6 N hydrochloric acid and heated for 30 minutes. After the iron was completely dissolved, the solution was diluted to 250 ml with DDI water. Five concentrations of Fe standards (0, 10, 40, 80, and 100 mg/L) were prepared by combining various volumes of the stock solution with 1 ml of hydroxylamine hydrochloric acid solution (1.256 g  $\text{BaSO}_4$  and 100 g hydroxylamine-HCl in 4% v/v HCl) and diluting to 10-ml with DDI water. The bipyridine solution (0.5 ml) was

then added and the solutions were analyzed as for Fe<sup>2+</sup>. Fe<sup>3+</sup> was calculated by subtracting the Fe<sup>2+</sup> concentration from the total Fe concentration.

A blank control was prepared in a similar manner as the standards except that the bipyridine solution was omitted and replaced with DDI water to correct for the background color of the Fe<sup>3+</sup>.

### 3.3.3 Chlorinated Ethenes

The concentrations of PCE, TCE, and *cis*-DCE were analyzed using a gas chromatograph (GC) (Hewlett Packard, model 5890 Series II Plus) equipped with a flame ionization detector (FID). The stainless-steel GC column was packed with 1% SP-1000 on 60/80 Carbopak-B (Supelco Inc., 3.2 mm x 2.44 m). Helium (Airgas East, Ultra purity carrier grade) was used as the carrier gas at a flow rate of 40 ml/min. Ultra purity carrier grade hydrogen and air were obtained from Airgas East and used at 60 ml/min and 260 ml/min, respectively, to maintain the FID. The injector and detector temperatures were set at 200°C and 250°C, respectively. As described by Gossett (1985), the initial oven temperature was 60°C with a hold time of 2 min, and then increased at a rate of 20°C/min to 150°C, following by an increase at a rate of 10°C/min to 200°C. Under these operating conditions, the overall runtime was 15.7 minutes with specific retention times of 7.1, 10.1, and 14.7 minutes for *cis*-DCE, TCE, and PCE, respectively. Output signals from the GC were evaluated using HP GC Chemstation software (Agilent Technologies, Rev.A.10.02).

To monitor the degradation of PCE and the production of daughter chlorinated ethenes, headspace samples (0.5 ml) were periodically withdrawn from the batch reactors containing strain BB1 growing on PCE using a 1-ml gastight syringe equipped with an on-off push-button valve (Dynatech, A-2 Pressure Lok) and sterile needle and manually injected onto the GC. The concentration of each compound was calculated by comparison with a calibration curve. Briefly, a calibration curve was prepared for each compound using different standard concentrations. The standards were prepared gravimetrically by adding different volumes of a stock methanol solution containing the chlorinated ethenes to 6 ml of DDI water in an amber vial closed with a Teflon septum and crimp cap. The stock methanol solution was prepared gravimetrically by adding neat PCE, TCE, and *cis*-DCE to approximately 10 ml of methanol in an amber vial sealed with a Teflon septum. The standards were incubated and shaken for 3 hours in the dark at 30°C before 0.5 ml of headspace volume was withdrawn and injected onto the GC. The standard calibration curves were generated by plotting the aqueous concentration of the chlorinated compound as a function of the peak area. The aqueous concentrations were obtained from the following relationship:

$$M_t = C_w V_w + C_g V_g = C_w (V_w + H_C V_g) \quad (3.1)$$

where  $M_t$  is the total mass of the chlorinated compound [M],  $C_w$  is the aqueous concentration of the compound [ $\text{ML}^{-3}$ ],  $V_w$  is volume of aqueous phase [ $\text{L}^3$ ],  $C_g$  is the concentration of the compound in the gas phase [ $\text{ML}^{-3}$ ],  $V_g$  is the headspace volume



[L<sup>3</sup>], and H<sub>C</sub> is the dimensionless Henry's constant of the given compound (Table 3.2) at 30°C.

Table 3.2. Henry's constants of chlorinated ethenes at 30°C (Gossett, 1987)

Compound	Henry's Constant (H <sub>c</sub> )
PCE	0.190
TCE	0.491
<i>cis</i> -DCE	0.917

### 3.3.4 Biomass

The biomass concentration in the source culture used to inoculate the batch reactors was measured using one of two colorimetric protein assays, the Quanti Pro Bicinchoninic acid (BCA) and Bradford protein assays, which were selected based on their compatibility with the strain GS-15 and strain BB1 media compositions, respectively. The <sup>14</sup>C-based method used for measuring biomass in the batch experiments (described above) could not be used with the source culture, because the cultures were not grown with <sup>14</sup>C-labeled acetate.

Prior to protein analysis, 1-ml of cell suspension was withdrawn from a source culture using a sterile needle and syringe and transferred to a screw-cap microcentrifuge vial (Biospec Products Inc., 3 ml). Cell lysis was performed mechanically for 3 minutes using a Mini-BeadBeater-8 (Biospec Products, Inc.) after the addition of approximately 2 ml glass beads (Biospec Products Inc., 0.2 mm) to the sample vial. Gravitational separation of protein from the beads was achieved by letting the sample stand for 10 minutes at ambient temperature before the supernatant was collected for protein analysis. Standards were prepared by dissolving bovine serum albumin

(BSA) (Fisher Scientific) in DDI water and were treated in the same manner as the samples.

Strain GS-15 biomass was measured with the BCA protein assay (Sigma-Aldrich Inc.) following the manufacturer's instructions. Preparation of BCA reagent was performed by mixing 50 parts of bicinchoninic acid solution (containing bicinchoninic acid, sodium carbonate, sodium tartrate, and sodium bicarbonate in 0.1 N NaOH) with 1 part of copper(II) sulfate solution (4% w/v) in a screw-cap vial. Next 2 ml of color reagent was mixed with 0.1 ml of sample that had been diluted with DDI water to 1 ml in a disposable glass tube. The tube was incubated at 60°C for 30 minutes. The incubation time was 15-minutes longer than recommended by the manufacturer to help overcome the strong background color of the  $\text{Fe}^{3+}$ . A blank was also prepared for each set of the standards using fresh ferric citrate media and was treated with the color reagent. The reaction solution was transferred to a disposable cuvet after cooling to room temperature, and then the absorbance was measured at 562 nm with a spectrophotometer (HACH, model DR/4000V).

Strain BB1 protein samples were analyzed using the Bradford method (Bradford, 1976). The assay was performed following the instructions given by the manufacturer. The sample or standard was combined with the Bradford reagent (Sigma-Aldrich) in a 1:1 (v/v) ratio. The mixture was incubated at ambient conditions for 45 minutes and then transferred to a disposable cuvet (Fisher Scientific) before measuring its absorbance (595 nm) with a spectrophotometer (HACH, model

DR/4000V). The concentration of protein was calculated by comparing the absorbance with a calibration curve prepared using BSA.

### 3.4 Mathematical Modeling

#### 3.4.1 Model of Microbial Respiration

In this study, a previously-described model of microbial respiration (Jin and Bethke, 2003) is used to gain insight into the importance of kinetic and thermodynamic factors in controlling the acetate threshold concentrations for each TEAP. The model is general and can be used to describe all respiratory processes, including those evaluated in this study.

Jin and Bethke's respiration model incorporates both thermodynamic and kinetic terms according to

$$v = k[X]F_T F_D F_A \quad (3.2)$$

where  $v$  is the reaction rate ( $\text{ML}^{-3} \text{T}^{-1}$ ),  $k$  is the intrinsic reaction rate ( $\text{T}^{-1}$ ),  $X$  is the biomass concentration ( $\text{M}_x \text{L}^{-3}$ ),  $F_T$  is a thermodynamic factor (unitless), and  $F_D$  and  $F_A$  (both unitless) are kinetic factors of the electron-donating and -accepting half-reactions, respectively.

The thermodynamic factor  $F_T$  is expressed as

$$F_T = 1 - \exp\left(\frac{\Delta G + m\Delta G_p}{\chi RT}\right) \quad (3.3)$$

where  $\Delta G$  is the free energy change of the redox reaction (kJ/mol);  $\Delta G_p$  is the free energy change required for synthesis of 1 M of ATP (50 kJ/mol; White, 1955);  $m$  is the molecules of ATP synthesized per mole of electron donor oxidized; and  $\chi$  is defined by Jin and Bethke as "the ratio of the free energy change of the overall reaction to the sum of the free energy changes for each elementary step". Essentially  $\chi$  reflects the number of times the rate-limiting step occurs during respiration. When an electron acceptor is reduced extracellularly, as in the case of solid-phase electron acceptors, the transfer of electrons to the external electron acceptor is the rate-limiting step (Jin and Bethke, 2003).

The kinetic factors of the electron donating and accepting species are expressed as

$$F_D = \frac{[D]_{D}^{\beta_D}}{[D]_{D}^{\beta_D} + K_D [D^+]_{D^+}^{\beta_{D^+}}} \quad (3.4)$$

and

$$F_A = \frac{[A]_{A}^{\beta_A}}{[A]_{A}^{\beta_A} + K_A [A^-]_{A^-}^{\beta_{A^-}}} \quad (3.5)$$

respectively, where  $K_D$  and  $K_A$  are constants that reflect the standard free energy changes of the electron-donating and electron-accepting reactions; and  $\beta_D$ ,  $\beta_{D^+}$ ,  $\beta_A$ , and  $\beta_{A^-}$  are unitless exponents whose values are determined by "details of the mechanism of electron transport" but are often assumed to be unity, as is the case in this study (Jin and Bethke, 2003).

$F_T$  values can range from 0 to 1. When the thermodynamic driving force of a reaction approaches zero,  $F_T$  is equal to 0 and the microbial reaction will cease. Under these conditions, thermodynamics control the threshold concentration of the limiting substrate. Similarly, the values of  $F_D$  and  $F_A$  can range from almost 0 to 1, depending upon the concentrations of the substrates and end products. When the substrate concentrations are high and the product concentrations are low,  $F_D$  and  $F_A$  approach 1 and the growth rate is not limited by kinetics. If end products accumulate to high levels and the limiting substrate concentration is low,  $F_D$  or  $F_A$  approaches 0, which means the threshold is controlled by kinetics. Evaluation of the  $F_T$ ,  $F_D$ , and  $F_A$  values when the limiting substrate concentration reaches the threshold value in the batch reactors was used in this study to determine whether kinetic and/or thermodynamic factors control the acetate threshold concentration for a given TEAP.

To calculate  $F_D$  and  $F_A$  values in the batch reactors as a function of time, estimates of the constants  $K_D$  and  $K_A$  were needed. In this research,  $[D^+]$  ( $\text{HCO}_3^-$ ) was assumed to be constant in the batch reactors because of the high concentration of  $\text{HCO}_3^-$  added to the media and its constant pH. Therefore, the lumped parameter  $K'_D$  can be defined as the product of  $K_D$  and  $[D^+]$ . When strain GS-15 was growing on excess levels of  $\text{Fe}^{3+}$ ,  $F_A$  and  $F_T$  were equal to 1 and Equation 3.2 was used to fit  $k$  and  $K'_D$  to the measured values of  $[D]$  (acetate). Likewise, acetate was provided in excess so that  $F_D$  and  $F_T$  would remain relatively constant and Equation 3.2 could be used to fit  $k$  and  $K_A$  to the measured values of  $[A]$  and  $[A^-]$ . The  $k$  values measured under electron-donating and electron-accepting reactions were quite similar and the values reported below reflect the averages of the values fit under the two sets of conditions. The

experimental data  $[D]$ ,  $[D^+]$ ,  $[A]$ , and  $[A^-]$  collected under dual substrate-limiting conditions (Table 3.1) were used to evaluate the  $k$ ,  $K'_D$ , and  $K_A$  parameter fit under single substrate-limiting conditions. The values of  $m$  and  $\chi$  were estimated from the literature as described below.  $\Delta G$ , which is needed to calculate  $F_T$  (Equation 3.3), was calculated from the measured  $[D]$ ,  $[D^+]$ ,  $[A]$ , and  $[A^-]$  values and  $\Delta G^\circ_{30^\circ\text{C}}$ . The  $\Delta G^\circ_{f, 30^\circ\text{C}}$  values needed to calculate  $\Delta G^\circ_{30^\circ\text{C}}$  were determined using the van't Hoff equation:

$$\ln\left(\frac{K_{25}}{K_{30}}\right) = \left[\frac{\Delta H^\circ_{f, 25^\circ}}{R}\right]\left(\frac{1}{T_{25}} - \frac{1}{T_{30}}\right) \quad (3.6)$$

where  $K_{25}$  and  $K_{30}$  are the equilibrium constants at  $25^\circ\text{C}$  and  $30^\circ\text{C}$ , respectively;  $\Delta H^\circ_{f, 25^\circ}$  is the standard enthalpy of formation;  $T_{25}$  is 298.15 K; and  $T_{30}$  is 303.15 K.  $K_{25}$  was calculated according to:

$$K_{25} = \exp\left(\frac{-\Delta G^\circ_{f, 25^\circ}}{RT}\right) \quad (3.7)$$

After  $K_{30}$  was calculated from Equation 3.6,  $\Delta G^\circ_{f, 30^\circ}$  can be calculated according to:

$$\Delta G^\circ_{f, 30^\circ} = -RT \ln K_{30} \quad (3.8)$$

The  $\Delta H^\circ_{f, 25^\circ}$  and  $\Delta G^\circ_{f, 25^\circ}$  values of reactants and products used for the calculation and the calculated  $\Delta G^\circ_{f, 30^\circ}$  are summarized in Table 3.3 below.

Table 3.3. Thermodynamic values of various chemical species used in current study.

Compound	$\Delta G_f^\circ$ at 25°C (kJ/mol) <sup>a</sup>	$\Delta H_f^\circ$ at 25°C (kJ/mol) <sup>a</sup>	$\Delta G_f^\circ$ at 30°C (kJ/mol)
Fe(II)	-84.9	-87.9	-84.9
Fe(III)	-10.6	-47.7	-9.9
MnO <sub>2</sub>	-464.9	-519.8	-464.0
Mn(II)	-227.7	-223.1	-227.7
NO <sub>3</sub> <sup>-</sup>	-110.6	-206.6	-109.0
NH <sub>4</sub> <sup>+</sup>	-79.5	-132.8	-78.6
SO <sub>4</sub> <sup>2-</sup>	-742.2	-907.7	-739.4
HS <sup>-</sup>	12.6	-17.7	13.1
S <sub>0</sub>	0.0 <sup>b</sup>	0.0 <sup>b</sup>	0.0
PCE	29.6 <sup>c</sup>	-52.0 <sup>c</sup>	31.0
TCE	21.7 <sup>c</sup>	-47.9 <sup>c</sup>	22.9
<i>cis</i> DCE	23.2 <sup>c</sup>	-35.1 <sup>c</sup>	24.2
CH <sub>3</sub> COO <sup>-</sup>	-369.4	-486.0	-367.5
HCO <sub>3</sub> <sup>-</sup>	-587.2	-691.3	-585.5
ATP	-2098.0 <sup>d</sup>	-2992.9 <sup>d</sup>	-2083.1
ADP	-1234.4 <sup>d</sup>	-2001.9 <sup>d</sup>	-1221.5
Pi	-1058.6 <sup>d</sup>	-1301.2 <sup>d</sup>	-1054.5

<sup>a</sup>From Snoeyink and Jenkins (1980), unless noted otherwise.

<sup>b</sup>From Stumm and Morgan (1996).

<sup>c</sup>From Heimann and Jakobsen (2006).

<sup>d</sup>From Alberty (1998).

### 3.4.2 Estimation of $m$ and $\chi$

For strain GS-15 growing on iron,  $m$  was estimated to be 0.45 mol ATP per mol acetate based on the predicted theoretical energy yields of strain GS-15, which range from 0.3 to 0.6 mol ATP per mol acetate (Champine et al., 2000).

According to Champine et al. (2000), the transfer of electrons to ferric citrate by strain GS-15 is assumed to occur externally. Therefore, it is assumed to be the rate-limiting step for the purposes of this study. The reduction of Fe(III) presumably occurs when a terminal oxidase receives an electron from a cytochrome, such as cytochrome  $c_7$  (Champine et al., 2000). Because the reduction of Fe(III) to Fe(II)

involves one electron and the oxidation of acetate to CO<sub>2</sub> yields 8 electrons,  $\chi$  is assumed 8 for strain GS-15 growing on ferric citrate.

For strain BB1 growing on PCE,  $m$  was estimated based on the presumption that the yield of the cell is directly proportional to the amount of ATP produced (Russell and Gregory, 1995). Bauchop and Eldent (1960) correlated biomass production with ATP availability from several anaerobic microbes and found the value ranged from 8.3 to 12.6 g biomass per mol ATP. In this study, an average value of 10.5 g biomass per mol of ATP was used. According to Sung et al. (2003), strain BB1 yields 1 g of protein per 0.95 mol of acetate. With the assumption that protein accounts for 60% of the biomass, this yield is equivalent to 1.67 g biomass per mol acetate. Thus,  $m$  for strain BB1 is estimated to be 0.16 mol ATP per mol acetate.

The estimation of  $\chi$  for strain BB1 mediating PCE dechlorination was based on the assumption that proton translocation is the rate-limiting step. According to Hägglom and Bossert (2003), the transfer of electrons from the donating species to the electron accepting reductive dehalogenase occurs in the cytoplasmic membrane and cytochromes and quinones are electron transfer components found in the cell membrane of dehalorespiring bacteria. The components of the electron transport system have not been reported for strain BB1. However, a *c*-type cytochrome was found in *Desulfuromonas chloroethenica*, which is 97.5% similar to strain BB1 on the basis of their 16s rRNA sequences (Hägglom and Bossert, 2003), and menaquinones have been detected in the membrane of *Dehalobacter restrictus*, another strain capable of respiring PCE and TCE to cisDCE (Krumholz, 1997). It is also assumed



that the ratio of protons translocated to electrons transferred to PCE in strain BB1 is 1:1 as observed for *Desultomonile tiedjei* and *Dehalobacter restrictus* (Krumholz, 1977). Therefore,  $\chi$  for strain BB1 is assumed to be 8 per mole of acetate oxidized.

### **3.5 Microcosm Experiment**

In addition to the small-scale batch experiments conducted to fit the respiration model parameters and measure thresholds in pure cultures, a related study was undertaken to evaluate the thresholds under different dominant TEAPs in undefined environmental samples. This study was undertaken using 1.6 L microcosms containing anaerobic sediment and groundwater collected at Aberdeen Proving Ground, MD. The microcosm study was initiated by Gayle Davis, and the detailed procedures used for sediment collection, preparation of the microcosms, characterization of the sediment TEAPs, related analytical methods, and initial results obtained under methanogenic condition have been described (Davis, 2005). Additional analyses of acetate thresholds under methanogenic and sulfate-reducing conditions subsequent to the experiments completed by Gayle Davis are described below. An enzymatic method used for quantification of unlabeled acetate that was used in the microcosm experiments is also described below.

#### **3.5.1 Use of Microcosms to Evaluate Acetate Thresholds under Methanogenic Conditions**

##### **3.5.1.1 General Experimental Approach**

Davis (2006) described the results obtained during the metabolism of two repeated additions of acetate from day 0 to day 54 in duplicate microcosms under

methanogenic conditions. Three additional spikes of acetate that ranged from approximately 900  $\mu\text{M}$  and up to 2,900  $\mu\text{M}$  were subsequently added to duplicate reactors. The acetate concentration was monitored until it reached a threshold. The operational definition of a threshold used in this thesis is the average of five measured concentrations that can be fit with a line with a slope not significantly different than zero, based on the P test at the 95% confidence interval.

On day 207, after the 5th addition of acetate to the microcosms under methanogenic conditions, the reactors were again amended with 1 mM of acetate (from a 0.35 M stock solution) along with 2.5 mM of sulfate (from a 1.27 M stock solution) to promote sulfate-reducing conditions. As discussed in greater detail below, when acetate reached a threshold concentration on day 303, 35% of the sulfate remained and methane continued to accumulate. Thus sulfate-reducing bacteria may not have controlled the acetate threshold. To inhibit the growth of methanogens and ensure that an acetate threshold could be measured under sulfate-reducing conditions the microcosms were amended with 2 mM of the specific inhibitor of methanogenesis, 2-bromoethanesulphonate (BES), from a stock solution (164 g/L of 2-bromoethanesulfonic acid, sodium salt) on day 308 (and subsequently on day 390). This was followed with the addition of approximately 2.5 mM of sulfate and 1.2 mM of acetate on day 311. Sulfate and sulfide were periodically monitored along with acetate,  $\text{H}_2$  and cumulative  $\text{CH}_4$ . The monitoring of  $\text{H}_2$  and  $\text{CH}_4$  was continued under sulfate-reducing conditions, to collect information on  $\text{H}_2$  thresholds and evaluate the effectiveness of the inhibition of the methanogens.

### 3.5.1.2 Analytical Methods

Cumulative methane and hydrogen in the headspace were monitored regularly throughout the entire microcosm study, using methods described by Davis (2006). Slurry samples were also treated according to Davis (2006) and analyzed for acetate using the enzymatic method described by King (1991). Briefly, AMP produced from an enzymatic reaction between acetate, ATP, and coenzyme A that is catalyzed by acetyl CoA synthase, was measured using the same HPLC system above except that an ion-exchange column was replaced with a C18 silica reverse-phase column (Supelcosil LC-18, 25cm x 4.6mm, 5µm silica particles).

The following description of the acetate analytical protocol was taken from Davis (2006):

"Initially, the mobile phase (1.3 ml/min) consisted exclusively of mobile phase A (0.1M  $\text{KH}_2\text{PO}_4$ ). Mobile phase B (90% Mobile A:10% methanol v/v) was provided according to the gradient outlined in Table 4.5. Adenosine monophosphate (AMP) eluted at approximately 13.7 minutes. This gradient run was continued for a total of 25 minutes to elute any additional proteins produced by the enzymatic reaction or present in the sample. At the conclusion of each injection, an 18 minute stabilization period was maintained with filtered deionized water prior to subsequent injections to avoid ghost peaks in subsequent injections. AMP was detected by monitoring UV absorbance at 254 nm using the Waters 996 Photodiode Array Detector. Empower

Software (Waters Corporation, 2000) was used for analysis and integration of the output signal from the HPLC...the acetate analysis required the following stock solutions, which were prepared using deionized water: 10 mM adenosine triphosphate (ATP) (Sigma-Aldrich), 200 Lg/ml bovine serum albumin (Sigma-Aldrich), 10 mM Coenzyme A disodium salt (Fluka, 27593), and 20 U/ml Acetyl CoA synthase (Sigma, A1765)."

Sulfate was analyzed in 10-ml slurry samples obtained from the microcosm using the Hach turbidimetric method (method no. 680) and a Hach DR 2400 spectrophotometer. Five standards (0, 10, 20, 40, 60 mg/L  $\text{SO}_4^{2-}$ ) were prepared from a stock solution of sodium sulfate (0.1479 g  $\text{Na}_2\text{SO}_4/\text{L}$ ). The contents of a Sulfa Ver 4 reagent powder pillow (Hach) were added to the samples and blanks (prepared with DDI water) and swirled to mix before reacting for 5 minutes. A background reading was obtained by measuring the absorbance (450 nm) of the blank. The background absorbance was subtracted from the absorbance measured in the samples.

Sulfide was analyzed in 25-ml slurry samples using the Hach methylene blue method (method no. 690) and a Hach DR 2400 spectrophotometer. Five standards (0, 100, 200, 400, 700 mg/L  $\text{S}^{2-}$ ) were prepared from a stock solution of sodium sulfide (0.5989 g of clean and dry  $\text{Na}_2\text{S} \cdot 9\text{H}_2\text{O}/\text{L}$ ). 1 ml of sulfide 1 reagent (Hach) was added to the samples and blank using a 1-ml pipette and swirled to mix. Then 1 ml of sulfide 2 reagent (Hach) was added, and the samples were immediately inverted to mix, and allowed to incubate at room temperature. A pink color developed, and then

the solution turned blue if sulfide was present. The absorbance at 665 nm was measured in the blank and subtracted from the absorbance in the samples.

## Chapter 4

### Background Information, Result, and Discussion

This chapter provides specific background information related to the use of electron acceptor concentrations as a monitoring tool to assess bioremediation in a contaminated anaerobic system. Following the background information, the experimental results from the pure culture studies are presented and discussed, along with the evaluation of a microbial respiration model. Finally, the results from the microcosm study are presented, discussed, and compared to the results from the pure culture study to investigate the possible application of this study's results to actual contaminated sites.

#### 4.1 Background Information

In anaerobic subsurface environments, hydrogen and organic acids are commonly found as intermediate metabolic products, resulting from the fermentation of organic matter. The organic matter can be naturally available on site or come from anthropogenic sources such as petroleum hydrocarbon leakage. Hydrogen and organic acids can then be used as energy sources (e.g., electron donor) for microbial respiratory processes (Rittmann and McCarty, 2001). Along with these electron donors, several terminal electron acceptors are also commonly found in groundwater systems including oxygen,  $\text{NO}_3^-$ , Fe(III), and  $\text{SO}_4^{2-}$ , and  $\text{CO}_2$  (Chapelle et al., 2002). In order to obtain free energy to support growth, respiratory bacteria couple the oxidation of a given electron donor to the reduction of an electron acceptor.

Theoretically, considering thermodynamics only, the use of electron acceptors that yield the most negative free energy change will occur first, followed by the ones that yield less negative free energy, in sequential order. The stoichiometry and standard Gibbs free energy ( $\Delta G^\circ$ ) change of these redox reactions under different terminal electron accepting processes (TEAPs), when acetate is used as the electron donor, are presented in Table 4.1 according to the energetically preferential order. Given this, it is expected based on thermodynamic considerations that a characteristic shift in the predominant electron accepting process (TEAP) will occur in a contaminant plume, with different TEAPs existing in an orderly succession (Figure 4.1), moving away from a source zone. Assuming there is a large amount of organic matter at the source, then near the source all of the most favorable electron acceptors will have been consumed, with only fermentation occurring. Moving down gradient, successively more favorable electron acceptors will become available, going from the least favorable to the most favorable, as the electron donor concentration decreases. This conceptual model of the spatial or temporal distribution of redox zones at a contaminated site can be used as monitoring and evaluation tool for on-going *in situ* bioremediation. One, a spatial or temporal change in the dominant TEAP can be an indicator of biological activity. Two, knowledge of the dominant TEAP is helpful in evaluating what microbial transformations of pollutants are possible under the existing conditions.

However, Lovley and Goodwin (1988) indicated that linking the ecological succession of TEAPs to biodegradation in the field can be technically challenging due to several different factors. For example, although various electron acceptors can be

Table 4.1 Overall redox reactions for acetate oxidation coupled to the reduction of various electron acceptors, along with the associated standard free energy of reactions (Free energy calculated from the standard free energies of formation of the products and reactants by assuming standard conditions except for pH 7).

TEAP	Overall Reaction	$\Delta G^{\circ}$ (kJ/reaction)
Oxygen reduction	$\text{CH}_3\text{COO}^- + 2\text{O}_2 = \text{HCO}_3^- + \text{CO}_2 + \text{H}_2\text{O}$	-849 <sup>a</sup>
Fe(III) reduction	$\text{CH}_3\text{COO}^- + 8\text{Fe}^{3+} + 4\text{H}_2\text{O} = 2\text{HCO}_3^- + \text{Fe}^{2+} + 9\text{H}^+$	-455 <sup>b</sup>
Denitrification	$\text{CH}_3\text{COO}^- + 1.6\text{NO}_3^- + 2.6\text{H}^+ = 2\text{CO}_2 + 0.8\text{N}_2 + 2.8\text{H}_2\text{O}$	-802 <sup>c</sup>
Mn(IV) reduction	$\text{CH}_3\text{COO}^- + 4\text{MnO}_2 + 7\text{H}^+ = 4\text{Mn}^{2+} + 2\text{HCO}_3^- + 4\text{H}_2\text{O}$	-737 <sup>a</sup>
Nitrate reduction	$\text{CH}_3\text{COO}^- + \text{NO}_3^- + \text{H}^+ + \text{H}_2\text{O} = \text{NH}_4^+ + 2\text{HCO}_3^-$	-500 <sup>a</sup>
PCE Dechlorination	$\text{CH}_3\text{COO}^- + 2\text{PCE} + 3\text{H}_2\text{O} = \text{HCO}_3^- + \text{CO}_2 + 2\text{DCE} + 4\text{Cl}^- + 4\text{H}^+$	-439 <sup>d</sup>
Sulfate reduction	$\text{CH}_3\text{COO}^- + \text{SO}_4^{2-} = 2\text{HCO}_3^- + \text{HS}^-$	-52 <sup>a</sup>
Methanogenesis	$\text{CH}_3\text{COO}^- + \text{H}_2\text{O} = \text{HCO}_3^- + \text{CH}_4$	-31 <sup>a</sup>

<sup>a</sup> From Lovley et al., 1988.

<sup>b</sup> From Liu et al., 2002.

<sup>c</sup> From Thauer et al., 1989.

<sup>d</sup> Calculated using standard enthalpy of formation from Table 3.3

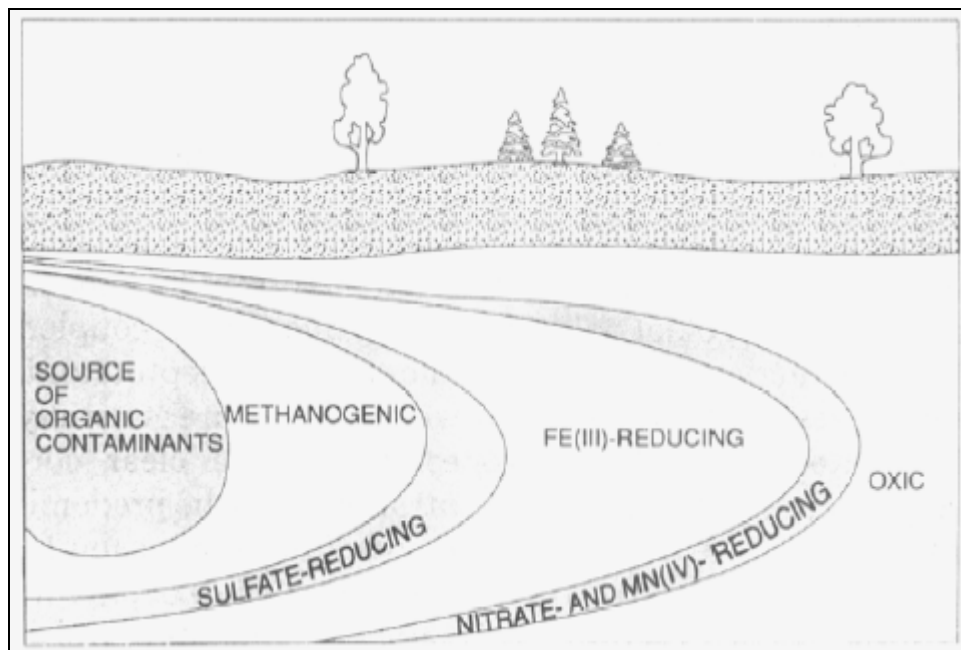


Figure 4.1. Distribution of predominant TEAPs in sequential order away from contaminant source beginning with methanogenesis, sulfate reduction, Fe(III) reduction, nitrate and manganese reduction, and aerobic oxidation, respectively (Lovley, et al., 1994).



found at a given site, the reduction of some of these compounds may not occur in the absence of bacteria that are capable of actively using them. Furthermore, delineation of redox zones can also be difficult when some electron acceptors or their reduced products migrate away from the active zone. Finally, there are a number of technical difficulties associated with measurement of these compounds under anaerobic subsurface conditions.

Therefore, Lovley and Goodwin (1988) suggested the use of characteristic hydrogen threshold concentrations to indicate the predominant TEAP. The substrate threshold is defined as a concentration at which the substrate cannot be metabolized any further (Lovley and Goodwin, 1988). In general, microbially mediated catabolic processes require an input of some energy (ATP), and the substrate threshold represents the minimum amount of derived energy below which microbial metabolism cannot be sustained (Hopkins et al., 1995; Warikoo et al., 1996; Hoehler et al., 1998). According to this concept, one group of hydrogenotrophic microorganisms can competitively exclude the other hydrogenotrophic microbes that use less favorable TEAPs by maintaining the hydrogen concentration at the level below which the metabolism of the other group(s) cannot be maintained. Theoretical analysis and several field studies have demonstrated that such characteristic hydrogen thresholds do exist and that the threshold  $H_2$  values decrease as the free energy available from the redox reaction between hydrogen and associated electron acceptors increases (Lovley and Goodwin, 1988; Chapelle et al., 1996; and Hoehler et al., 1998). For example, Chapelle et al. (1997) showed that the characteristic hydrogen threshold observed in the field could range between 5-30 nM under methanogenesis, 1-4 nM

under sulfate reduction, 0.2-0.8 nM under Fe(III) reduction, and less than 0.1 nM under nitrate reduction. However, several factors affect accurate quantification of hydrogen concentration in the subsurfaces. These factors include difficulties in pumping and handling samples from subsurface for H<sub>2</sub> analysis, the detection limits of instrumentation for H<sub>2</sub> analysis such as gas chromatography, and solute concentration and temperature effects due to hydrogen's gaseous nature, among others (Chapelle et al., 1997). Clearly, an alternative, accurate, reliable and rapid method to replace use of hydrogen thresholds for indicating shifts in TEAPs would be useful.

One alternative to hydrogen, is to use organic acids such as acetate as monitoring tool for bioremediation (Barcelona et al., 1993; and Cozzarelli et al., 1994). As reviewed by Seagren and Becker (1999), acetate plays a similar role as hydrogen during anaerobic degradation of organic compounds. By using the concept of  $S_{\min}$ , the concentration below which biomass cannot be maintained at steady-state (discussed further below), the authors predicted that acetate threshold concentrations ( $S_{\min}^* = S_{\min}/K_s$ ) will increase as the terminal electron acceptor become more reduced (Table 4.2). Indeed, several studies have shown that acetate threshold concentrations existed under different TEAPs. For example, acetate threshold concentrations could range between 0.069-1.18 mM under methanogenic conditions (Westermann et al., 1989), 2-50  $\mu$ M under sulfate reducing conditions (McMahon and Chapelle, 1991; and Chapelle and Lovley, 1992), and 0.5-3  $\mu$ M under Fe(III) reducing conditions (Chapelle and Lovley, 1992). These evaluations further suggest that acetate thresholds can potentially be a useful indicator of the dominant TEAP or a shift in TEAPs.

Table 4.2  $S_{\min}^*$  values predicted for various TEAPs (Seagren and Becker, 1999)

TEAP	$S_{\min}^* = S_{\min}/K_s$
O <sub>2</sub> /H <sub>2</sub> O	0.00125
Fe <sup>3+</sup> /Fe <sup>2+</sup>	0.0013
NO <sub>3</sub> <sup>-</sup> /N <sub>2</sub>	0.00133
SO <sub>4</sub> <sup>-</sup> /HS <sup>-</sup>	0.021
CO <sub>2</sub> /CH <sub>4</sub>	0.038

Finally, although the focus until this point has been on thermodynamic considerations, it is important to realize that the substrate threshold concentrations are controlled by both thermodynamic and kinetic factors. As noted above, thermodynamic controls on thresholds are a function of the amount of free energy available from a chemical transformation to support microbial growth. However, kinetic factors may also play a key role in controlling substrate metabolism by microorganisms, especially at low concentrations (Watson et al., 2003; Jin and Bethke, 2002). In particular, if kinetic factors cause the substrate utilization rate to approach zero, a threshold will be reached. Not understanding this could result in a misinterpretation of field data. An example of this comes from the study conducted by Vroblesky et al. (1997), in which the authors evaluated the connection between the hydrogen and acetate threshold concentrations in a groundwater contaminant plume. The authors concluded that there was no connection between the hydrogen and acetate thresholds. However, the study neglected the potential role of kinetic factors in controlling substrate thresholds, and used an analytical method with a high detection limit to measure the H<sub>2</sub> concentrations, which were used to infer the existence of various TEAPs. It is possible that the thresholds in this study were controlled by kinetic factors and that the results from the H<sub>2</sub> measurements did not accurately represent the TEAPs, both of which could have accounted for the lack of

correlation with the acetate data. Therefore, to be able to interpret acetate threshold results in a meaningful manner, the effect of thermodynamic and kinetic governing factors on microbial metabolism should also be investigated. The specific effects of these factors on microbial metabolism are discussed in further detail above, in Section 3.4.1, on the use of the microbial respiration model.

## **4.2 Results and Discussion**

### **4.2.1 Acetate Thresholds in Pure Culture Study**

Acetate thresholds were evaluated in two pure cultures of acetotrophs that can utilize different TEAPs. Thresholds were determined for three TEAPs in each of the two pure cultures. This made it possible to independently evaluate both the effects of the dominant TEAP (i.e., thermodynamics) and culture characteristics (i.e., kinetics) on acetate thresholds.

#### **4.2.1.1 Results Obtained with *Geobacter metallireducens***

The acetate threshold experiments with strain GS-15 were evaluated under Fe(III)-, Mn(IV)-, and NO<sub>3</sub><sup>-</sup>-reducing conditions using an initial acetate concentration of 2.5 mM. The trends of acetate depletion as a function of time for each of the three TEAPs are presented in Figure 4.2. Acetate concentrations were somewhat variable among the replicates particularly during the lag and exponential growth phases. This behavior was observed under each TEAP and primarily reflects differences in the

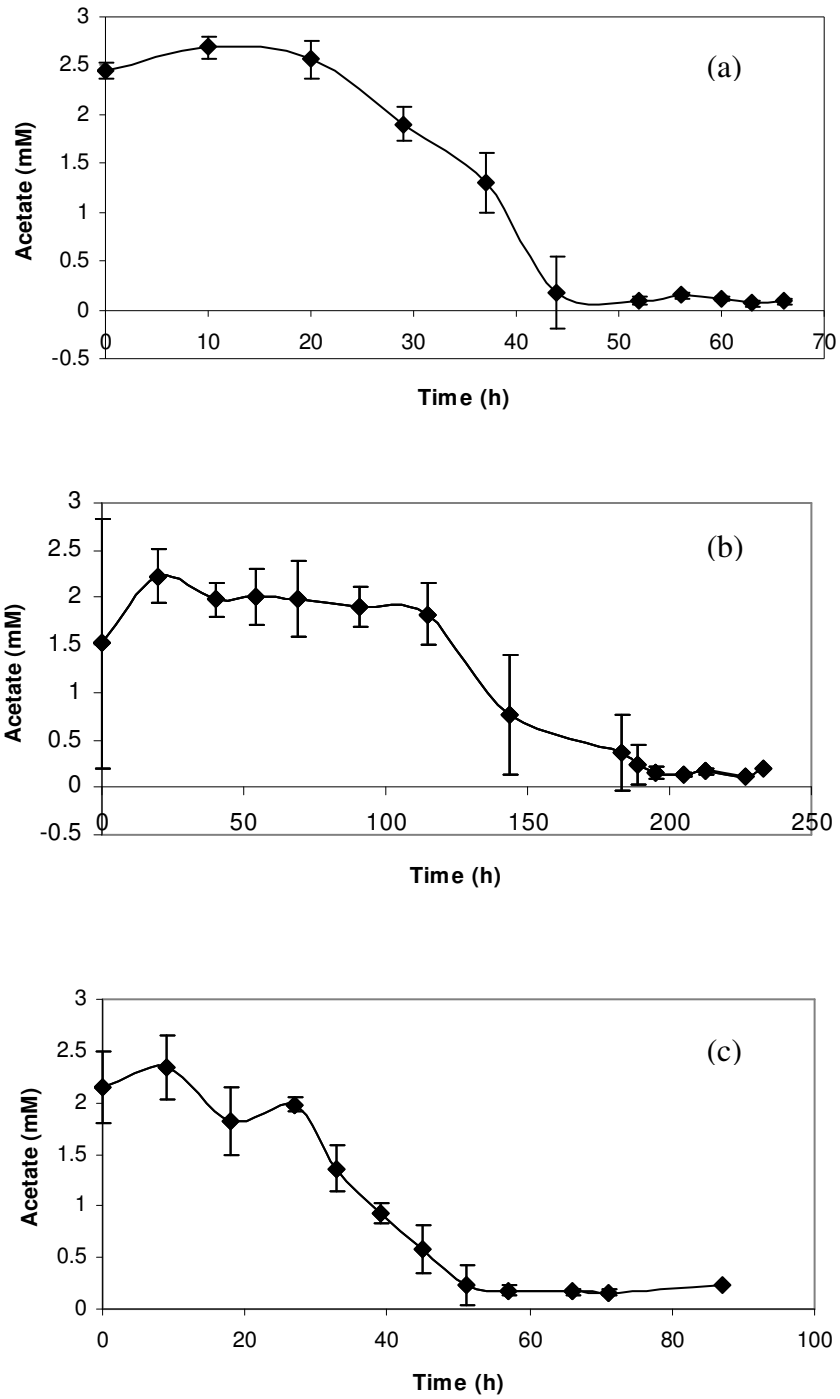


Figure 4.2. Acetate depletion curves for strain GS-15 growing on 2.5 mM of acetate as the electron donor and (a) 50 mM Fe(III), (b) 25 mM Mn(IV), and (c) 6.25 mM NO<sub>3</sub><sup>-</sup>. Each data point represents the average acetate concentration in triplicate batch reactors. Error bars represent ± one standard deviation.

length of the lag period in the different replicates. This variability is typical of batch cultures (Sommer et al., 1998). However, for a given TEAP, the student's t test ( $\alpha = 0.05$ ) was used to compare acetate threshold concentrations in the replicate reactors. Based on this analysis the differences in the acetate thresholds in the replicates were not significant ( $\alpha = 0.05$ ). However, there were significant differences between the thresholds measured under different TEAPs based on student's t test analysis ( $df=3$ ;  $\alpha=0.05$ ) using the average acetate concentrations from the last five measurements in each experimental condition. Specifically, the lowest acetate threshold was 111  $\mu\text{M}$  ( $P = 0.0054$ ), which was observed under Fe(III)-reducing conditions, followed by 154  $\mu\text{M}$  ( $P = 0.0095$ ) and 170  $\mu\text{M}$  ( $P = 0.02977$ ), under Mn(IV)- and  $\text{NO}_3^-$ -reducing conditions, respectively. In the experiment conducted under Fe(III)-reducing conditions, acetate was re-spiked into two of the batch reactors to ensure that the threshold was not due to limitation by some other growth factor(s). Growth in both of the re-spiked batch reactors resumed after the addition of approximately 1 mM of acetate, as indicated by the rapid depletion of acetate (data not shown). This confirmed that the acetate threshold concentration was only the result of limited amounts of acetate.

#### **4.2.1.2 Results Obtained with *Desulfuromonas michiganensis***

In the experiments conducted with strain BB1, Fe(III), PCE, and  $\text{S}^0$  were provided as electron acceptors at concentrations of 10 mM, 0.5 mM, and 2.5 mM, respectively, and acetate was provided as the electron donor at initial concentrations of 0.5, 0.1,

and 0.25 mM, respectively. The acetate depletion curves of strain BB1 growing on each of the electron acceptors are presented in Figure 4.3.

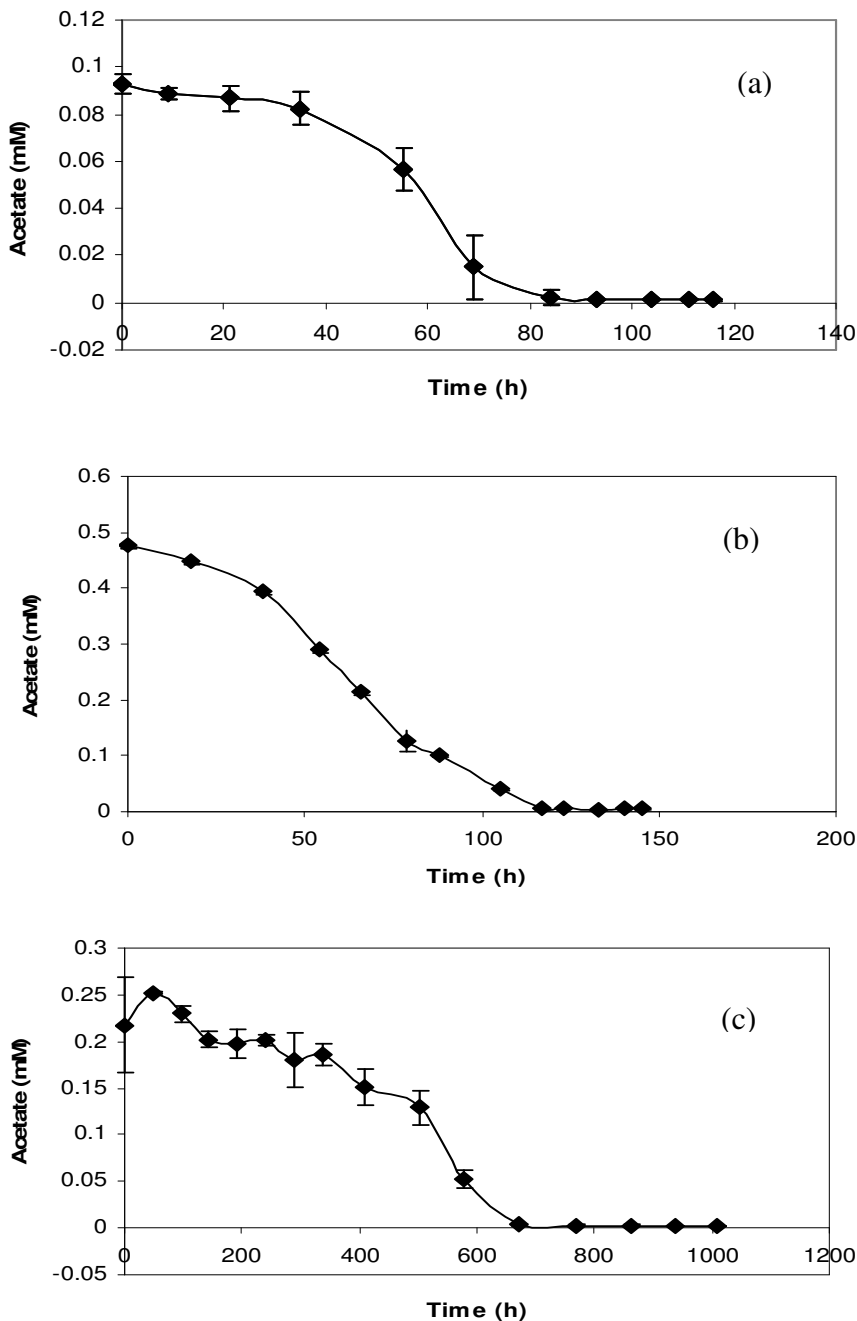


Figure 4.3. Acetate depletion curves for strain BB1 growing on (a) 0.1 mM of acetate as the electron donor and 0.5 mM PCE, (b) 0.25 mM of acetate and 2.5 mM  $S^0$ , and (c) 0.5 mM of acetate and 10 mM Fe(III). Each data point represents the average acetate concentration in triplicate batch reactors. Error bars represent  $\pm$  one standard deviation.

Similar to the results obtained with strain GS-15, there was substantial variation in the onset of acetate metabolism in the strain BB1 reactors growing on different TEAPs. As a result, there was some variability in the acetate concentrations measured in the lag and exponential growth phases. However, the acetate thresholds measured in the individual replicates, which were determined by calculation of the mean of the last five measurements, were not statistically different when analyzed with the student's t test ( $\alpha=0.05$ ). On the other hands, as with strain GS-15, significant differences were observed in the acetate thresholds determined under different TEAPs. Acetate threshold concentrations of 5.07  $\mu\text{M}$  ( $P = 0.1812$ ), 1.37  $\mu\text{M}$  ( $P = 0.0331$ ), and 2.73  $\mu\text{M}$  ( $P = 0.1023$ ), were measured under Fe(III)-reducing, PCE-respiring, and  $\text{S}^0$ -reducing conditions, respectively with strain BB1. To confirm that the acetate thresholds in strain BB1 were not the result of limitation by another growth factor, a test was performed using the cultures grown with PCE as the electron acceptor by re-supplying acetate to two of the batch reactors. Depletion of acetate occurred immediately after the addition of the substrate suggesting that the threshold levels were not due to limitation by other growth factors (data not shown).

#### **4.2.1.3. Factor Influencing Acetate Thresholds**

A summary of the acetate thresholds measured for the two pure cultures under the different TEAPs, along with the corresponding initial acetate concentrations is presented in Table 4.3. Also included in Table 4.3 is the  $\Delta G'_{30^\circ}$  for the reaction, which was calculated as described above, and  $\Delta G'_{30^\circ}$  at the conclusion of each experiment, which was calculated according to:



Table 4.3. Summary of acetate thresholds, initial acetate concentrations,  $\Delta G'_{30^\circ}$  and  $\Delta G'_{30^\circ}$  in the batch threshold experiments.

Culture	TEAP	$\Delta G'^{\circ}$ at 30°C (kJ/reaction)	Initial acetate concentration (mM)	Acetate threshold concentration ( $\mu$ M)	$\Delta G'$ at the conclusion of the experiment (kJ/reaction)
<i>Geobacter metallireducens</i> strain GS-15	Fe(III)	-457	2.5	111	-1108.6
			0.5	4.8	-1024.6
	Mn(IV)	-792	2.5	154	-1085.6
	NO <sub>3</sub> <sup>-</sup>	-765	2.5	170	-821.6
<i>Desulfuromonas michiganensis</i> strain BB1	PCE	-439	0.1	1.37	-757.7
	S <sup>0</sup>	-60	0.25	2.73	-438.4
	Fe(III)	-457	0.5	5.07	-1025.3

$$\Delta G'_{30^\circ} = \Delta G'^{\circ}_{30^\circ} + RT \ln Q \quad (4.1)$$

where  $Q$  represents the reaction quotient.

Most of the literature on thresholds assumes that they are controlled by the thermodynamics of the energy reaction (Lovley and Goodwin, 1988; Westermann, 1989; McMahon and Chapelle, 1991; Chapelle and Lovley; 1992). Thus, as the free energy generated by a reaction increases, the threshold is expected to decrease. However, as shown in Table 4.3, the measured acetate thresholds did not follow the trends expected based on the  $\Delta G'^{\circ}_{30^\circ}$  values. For example, for strain GS-15, the greatest  $\Delta G'^{\circ}_{30^\circ}$  occurs under Mn(IV)-reducing conditions; however, the lowest threshold resulting from metabolism of 2.5 mM acetate was measured under Fe(III)-reducing conditions, which releases the least free energy of the three TEAPs examined using strain GS-15. Similarly, Fe(III)-reduction is the most

thermodynamically favorable TEAP evaluated using strain BB1, yet the highest threshold was observed with strain BB1 under Fe(III)-reducing conditions.

One factor that clearly does affect the experimental acetate threshold values is the initial acetate concentration. For example, for strain GS-15 under Fe(III)-reducing conditions when the initial acetate concentration was 0.5 mM, the threshold measured was much lower than the value with an initial acetate concentration of 2.5 mM (Table 4.3). Similarly, with strain BB1, the acetate thresholds measured trend with the initial acetate concentrations, going from the lowest threshold with the lowest initial acetate concentration, to the highest threshold with the highest initial concentration.

Interestingly, the acetate thresholds for GS-15 with an initial acetate concentration of 2.5 mM did correlate with the  $\Delta G'$  at the conclusion of the experiment, with the highest free energy value at the lowest threshold value and the lowest free energy value at the highest threshold (Table 4.3). However, this pattern did not hold true for Strain BB1.

Clearly, the acetate threshold concentrations measured in these experiments are not simply a function of the standard reaction thermodynamics. This is not surprising because, in addition to thermodynamics, kinetic parameters can influence thresholds. This can be readily understood by inspecting the equation for  $S_{\min}$  [ $M_s L^{-3}$ ] in batch or continuous-flow systems (Rittmann, 1987).  $S_{\min}$  is defined in continuous flow systems as the substrate concentration below which biomass cannot be maintained at steady-state. Therefore,  $S_{\min}$  can be considered as the steady-state threshold

concentration below which biomass washout occurs and can be calculated for Monod kinetics according to:

$$S_{min} = \frac{K_s b}{q_{max} Y - b} \quad (4.2)$$

where  $b$  is the decay coefficient [ $T^{-1}$ ],  $q_{max}$  is the maximum specific substrate utilization rate [ $T^{-1}$ ],  $Y$  is the true yield coefficient [ $M_x M_s^{-1}$ ],  $K_s$  is the half saturation coefficient [ $M_s L^{-3}$ ], which characterizes the affinity of microbes for the substrate, and the  $S$  and  $X$  subscripts denote limiting substrate and biomass, respectively. According to McCarty (1972),  $Y$  is a function of the free-energy change of the electron donor oxidation, and electron acceptor reduction half-reactions. Thus, the steady-state threshold  $S_{min}$  is a function of thermodynamic factors, which are captured by  $Y$ , and kinetic factors, including  $K_s$ ,  $q_{max}$ , and  $b$  (Seagren and Becker; 1999; Lovley and Goodwin, 1988).

The modified microbial respiration model of Jin and Bethke (2003) was used to evaluate the relative importance of kinetic and thermodynamic factors on the measured acetate thresholds in this study. As previously discussed, this model predicts the microbial respiration rates based on the rate constant ( $k$ ), the biomass concentration, a thermodynamic term ( $F_T$ ), and kinetic terms for the electron donor ( $F_D$ ) and acceptor ( $F_A$ ) (Equation 3.2). The values of  $F_T$ ,  $F_D$ , and  $F_A$ , can range from 0 to 1. According to Equation 3.2, if any of these terms approaches 0, the reaction will cease and the substrate will reach its threshold concentration. Thus, inspection of  $F_T$ ,

$F_D$ , and  $F_A$  during the threshold experiment can reveal whether thermodynamic or kinetic factors control the threshold.

For each organism, the additional data needed to calculate  $F_T$ ,  $F_D$ , and  $F_A$ , as well as the respiration rate ( $v$ ) were obtained for a single TEAP. The additional analyses were performed under Fe(III)-reducing conditions for strain GS-15 and under PCE-reducing conditions for strain BB1 with either an electron donor or electron acceptor limitation. The model predictions used to fit the  $K'_D$  values are also shown in Figure 4.4.  $[A]$  and  $[A^-]$  were assumed in the strain GS-15 threshold experiment and monitored in the strain BB1 experiment and used in the calculation of  $F_T$ , according to Equations 3.3 and 4.1.

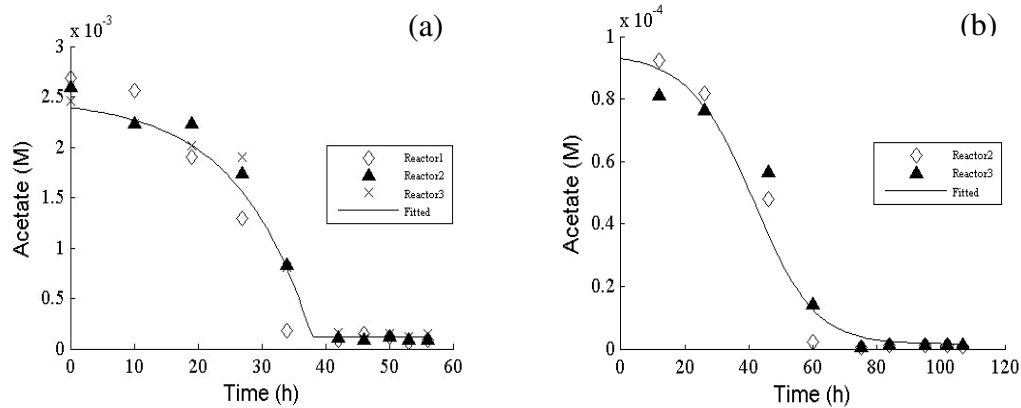


Figure 4.4. Acetate depletion data in triplicate or duplicate reactors of (a) strain GS-15 growing on Fe(III), and (b) strain BB1 growing on PCE under electron donor-limiting conditions. Data points represent individual experimental measurements. Lines represent the best fit of Equation 4.3 to the pooled experimental data.

$K_A$  values were fitted to electron acceptor accumulation curves obtained with excess acetate (Figures 4.5) and used along with the measured  $[A^-]$  values (Fe(II) or *cis*DCE plus TCE, for strains GS-15 and BB1, respectively) to calculate  $F_A$  (Equation 3.5).

Finally, biomass was also measured during the threshold experiments, which made it possible to estimate  $Y$ . The reported  $Y$  values were obtained by linear regression using the measured  $X_0$  values. The resulting estimated values of  $K'_D$ ,  $K_A$ ,  $k$ , and  $Y$  are summarized in Table 4.4. For strain GS-15,  $K'_D$ ,  $k$  and  $Y$  values were also fit to the acetate threshold experiments with an initial acetate concentration of 0.5 mM, as described above.

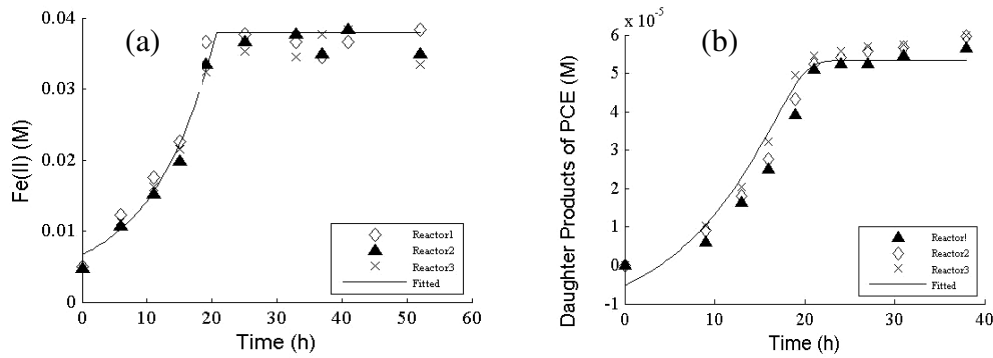


Figure 4.5. Reduced species accumulation data in triplicate reactors of (a) strain GS-15 growing on Fe(III), and (b) strain BB1 growing on PCE with excess acetate. Data points represent individual experimental measurements. Lines represent the best fit of Equation 3.5 to the pooled experimental data.

Table 4.4. Model parameter estimates fit to the experimental data

Culture	TEAP	$k$ (mol/ mg biomass.h)	$K'_D$ (M)	$K_A$ (M)	$Y$ (mol/mg biomass)
GS-15	Fe(III) Reduction (2.5 mM Acetate)	$1.4e-5$	$3.0e-7$	$1.6e-6$	$6.4e3$
GS-15	Fe(III) Reduction (0.5 mM Acetate)	$3.1e-5$	$2.7e-3$	N/A	$1.1e4$
BB1	PCE Dechlorination	$4.5e-5$	$9.6e-3$	$6.9e-2$	$5.0e3$

Surprisingly, the  $K'_D$  estimated for strain GS-15 with 2.5 mM acetate was nearly four orders of magnitude lower than the  $K'_D$  estimated for the same organism growing on 0.5 mM acetate. Because the  $K_D$  constant reflects the standard free energy change of the electron-donating half-reaction (Jin and Bethke, 2003), the estimated  $K'_D$  values should not be influenced by the initial acetate concentrations in this study. In fact, because  $K_D$  is a function of the standard free energy change of the electron donating half reaction, similar values should be obtained regardless of the TEAP or organism mediating the reaction. The  $K'_D$  value estimated for strain GS-15 growing on 0.5 mM acetate (0.0027 M) was close to the value estimated for strain BB1 growing on PCE (0.0096 M) and therefore was used to lieu of the  $K'_D$  value estimated with 2.5 mM acetate.

The fitted model parameteres obtained with strain GS-15 (2.5 mM acetate) and strain BB1 under electron donor and acceptor limiting condition were then validated by comparing the model predictions to the experimental data obtained under dual substrate-limiting conditions. The model predictions fit well with the experimental data obtained under iron-reducing conditions with strain GS-15 (Figure 4.6). However, the ability of the model to fit the data obtained under dual substrate-limiting conditions with strain BB1 was less satisfactory, although the model capture the general trend in the data (Figure 4.7). The poorer fit between the model and experimental data for the strain BB1 experiment is probably due to the experimental conditions. Specifically, the PCE concentration used in this experiment (0.5 mM) was very close to a level that has subsequently been shown to be toxic to strain BB1 (Huang, personal communication) and probably caused the culture to metabolize

acetate and PCE slower than predicted by the model. Nevertheless, the fitted parameters for strain BB1 shown in Table 4.3 were used to calculate  $F_T$ ,  $F_D$ , and  $F_A$ , and  $v$  values for strain BB1 growing on PCE.

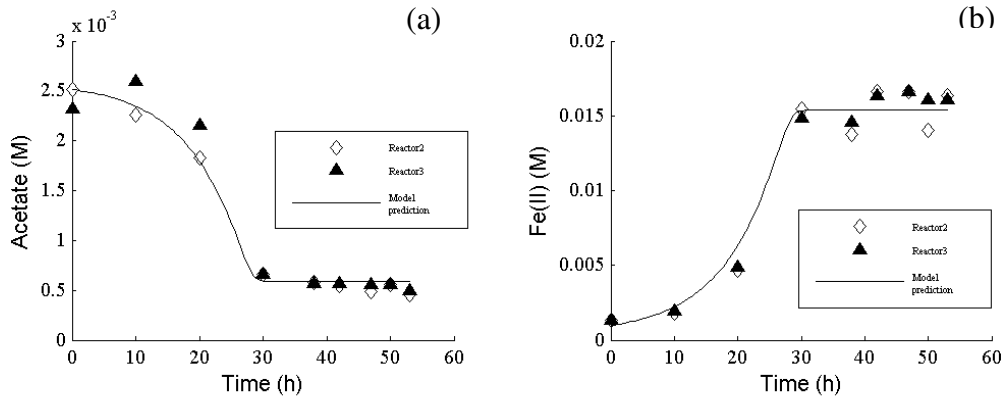


Figure 4.6. Comparison of experimental data and model predictions for strain GS-15 growing under dual substrate-limiting conditions: (a) acetate (2.5 mM) and (b) Fe(II) (from 20 mM Fe(III)). Each data point represents an individual measurement. Lines represent model predictions using  $K'_D$  and  $K_A$  values estimated at 2.5 mM acetate (Table 4.3).

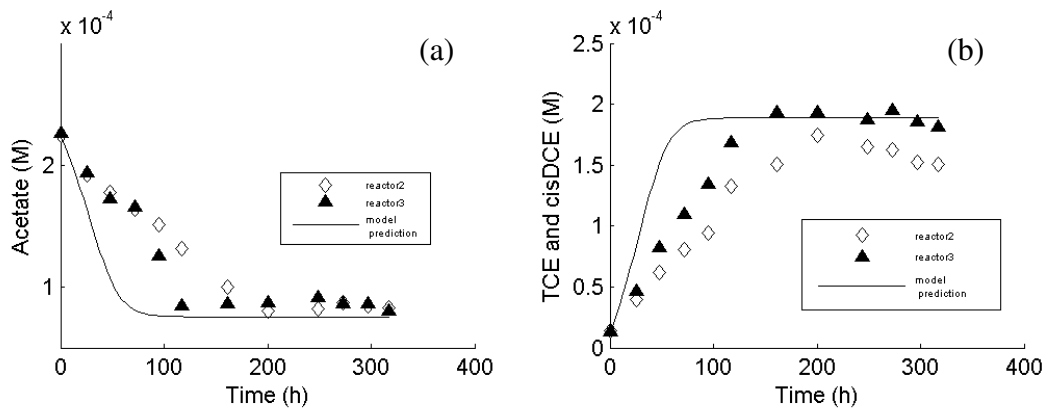


Figure 4.7. Comparison of experimental data and model predictions for strain BB1 growing under dual substrate-limiting conditions: (a) acetate (0.25 mM) and (b) aqueous concentration of daughter products of PCE (*cis*DCE and TEC). Each data point represents an individual measurement. Lines represent model predictions using  $K'_D$  and  $K_A$  values estimated at 0.1 mM and 0.25 mM acetate, respectively (Table 4.3).

The  $F_T$ ,  $F_D$ ,  $F_A$ , and  $v$  curves calculated for the electron donor limited cases shown in Table 4.3 are presented in Figure 4.8. As expected, the  $F_A$  term remained relatively constant at 1 during the threshold experiments for both strain GS-15 with 2.5 mM acetate (Figure 4.8 a) and strain BB1 with 0.1 mM acetate (Figure 4.8 c), because the electron acceptors were provided in excess.  $F_T$  terms also remained constant at 1 throughout the threshold for both strains for all three experiments shown in Figure 4.8. As described by Jin and Bethke (2005), it is not surprising for  $F_T$  to be equal to unity under TEAPs with relatively high redox potential. The free energy ( $\Delta G'$ ) calculated from the concentrations of D,  $D^+$ , A, and  $A^-$  always exceeded the energy conserved as ATP ( $m\Delta G_p = 22.5$  kJ/mol and 8 kJ/mol for strains GS-15 and BB1, respectively), even at the end of the experiment (Table 4.3). Thus, it appears that thermodynamic factor had little impact on the thresholds evaluated in this study. As described above, this finding is in contrast to conventional wisdom, which suggests that thermodynamics control threshold concentrations (Lovley and Goodwin, 1988; Westermann, 1989; McMahon and Chapelle, 1991; Chapelle and Lovley, 1992).

In contrast to  $F_A$  and  $F_T$ ,  $F_D$  was found to vary substantially during the course of the threshold experiments. For example, when strain GS-15 was growing on 2.5 mM acetate and the  $K'_D$  of 0.0027 M was used,  $F_D$  was initially 0.46 but decreased to 0.038 at the conclusion of the experiment suggesting that  $v$  and the acetate threshold under this condition were controlled by the kinetics of the electron donor. Similarly, when strain GS-15 was grown on Fe(III) and 0.5 mM of acetate,  $F_D$  dropped from approximately 0.8 to 0.0486 at the conclusion of the experiment suggesting that the microbial respiration rate and acetate threshold become kinetically controlled by the



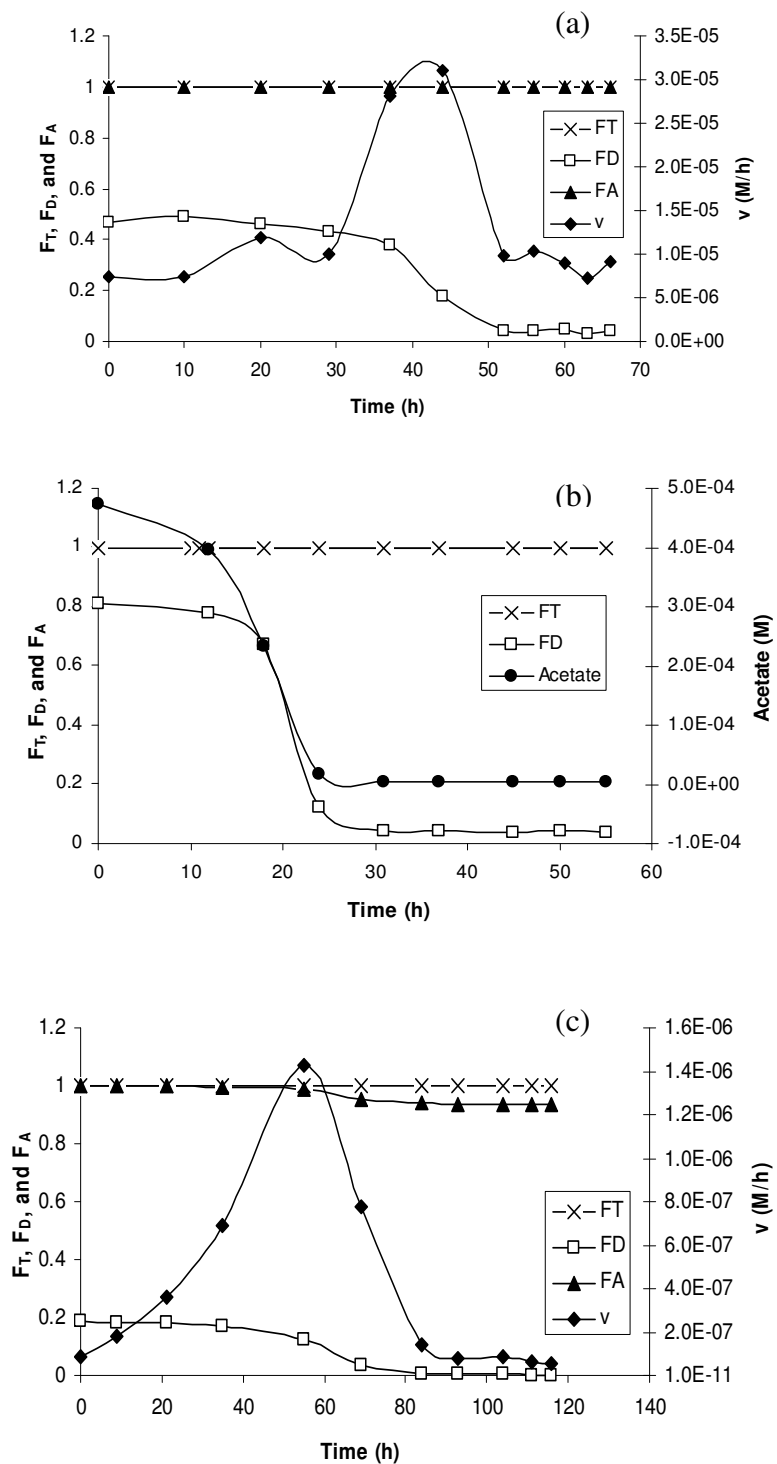


Figure 4.8: Evaluation of  $F_T$ ,  $F_D$ ,  $F_A$ , and  $v$ ; Strain GS-15 growing on Fe(III) using 2.5 mM acetate (a) and 0.5 mM (b) of acetate; and (c) Strain BB1 grown under limiting acetate using PCE as electron acceptor. The  $F_T$  values calculated for strain GS-15 were based on assumed concentrations of Fe(III) and Fe(II) because these values were not measured during the threshold experiments.

electron donor. It is possible that the kinetics of the electron acceptor ( $F_A$ ) species also played a key role in controlling  $v$  and the acetate threshold in this experiment. However,  $F_A$  was not investigated in this experiment.

$F_D$  for strain BB1 growing via PCE dechlorination with 0.1 mM of acetate exhibited a similar trend to that observed with strain GS-15 growing on Fe(III). A decrease in  $v$  was accompanied by a decrease in  $F_D$  (Figure 4.8(c)), while little or no change in the  $F_A$  and  $F_T$  values was observed. This suggests that the acetate threshold under PCE-dechlorinating conditions was also kinetically controlled by the electron donor.

It should be noted that in addition to thermodynamic and kinetic controls, other factors may influence acetate thresholds under certain conditions. For example, at low substrate concentrations, the necessary enzyme may not be fully expressed (Rittmann et al., 1994), especially in cultures that have previously been exposed to substrate rich environments. In addition, thresholds may sometimes reflect energy-requiring processes that are not associated with ATP synthesis. This could include the energy needed to take up substrates or, as noted by He and Sanford (2004), transport toxic compounds out of the cell cytoplasm.

Overall however, the results of the threshold experiments and the evaluations involving the respiration model indicated that acetate thresholds are controlled to a large extent by the kinetics of electron donor utilization.

Acetate thresholds have been measured under a variety of TEAPs in several previous studies using both pure cultures and environmental samples as summarized in Table 4.5. In general, the acetate thresholds measured with the pure cultures under Fe(III)citrate-reducing, nitrate-reducing, and dehalorespiring conditions in previous studies were in the nM range. These values are three to five times lower than the thresholds measured in the current study.

There are several potential explanations for the differences in the thresholds measured in the current study and those measured under the same TEAPs in other studies. The first reason is that, the organisms used in other studies (e.g. *Anaeromyxobacter dehalogenans* (He and Sanford, 2004) and *Geobacter lovleyi* (Sung et al., 2006)) likely have different kinetic attributes compared to strains GS-15 and BB1. The current study clearly demonstrates that kinetics play a role in determining thresholds. Thus, the differences in kinetic characteristics likely influenced the magnitude of the acetate thresholds measured in different studies. Second, the procedures and experimental conditions used in the different threshold determinations varied. For example, in the current study, thresholds were determined in cultures that exhibited unrestricted growth, while in other studies, the ratio of the initial substrate and biomass concentrations may have prevented growth (e.g. He and Sanford, 2004; Sung et al., 2006). It is possible that thresholds measured with resting cells, i.e., under extant condition, may be controlled by different factors than in growing cells. It is also very likely that differences in the methods used to measure the threshold concentration contributed to differences in the reported values. In particular, in the

Table 4.5. Previously reported and current acetate threshold concentrations under various TEAPs

TEAP	Electron acceptor	Environmental sample or pure culture	Initial acetate concentration (μM)	Acetate threshold (μM)	References
Mn(IV) reduction	MnO <sub>2</sub>	<i>Geobacter metallireducens</i>	2500	154	Current study
Fe(III) reduction	Fe(III) citrate	Sediment	100	0.5 ± 0.1	Lovley and Philips, 1987
		<i>Anaeromyxobacter dehalogenans</i>	10 to 40	< 0.001	He and Sanford, 2004
		<i>Geobacter lovleyi</i>	100	1.2x10 <sup>-3</sup> ± 5.0 x10 <sup>-4</sup>	Sung et al., 2005
		<i>Geobacter metallireducens</i>	2500	111	Current study
			500	4.8	Current study
		<i>Desulfuromonas michiganensis</i>	500	5.07	Current study
Nitrate reduction	NO <sub>3</sub> <sup>-</sup>	<i>Geobacter lovleyi</i>	100	3.6x10 <sup>-3</sup> ± 2.5 x10 <sup>-4</sup>	Sung et al., 2005
		<i>Geobacter metallireducens</i>	2500	170	Current study
Dehalorespiration	2-Chlorophenol	<i>Anaeromyxobacter dehalogenans</i>	10 to 40	0.069 ± 0.004	He and Sanford, 2004
	PCE	<i>Geobacter lovleyi</i>	100	3.0x10 <sup>-3</sup> ± 2.1x10 <sup>-3</sup>	Sung et al., 2005
	PCE	<i>Desulfuromonas michiganensis</i>	100	1.37	Current study
Sulfate reduction	SO <sub>4</sub> <sup>2-</sup>	Sediment	N/A	2.2 ± 0.2 <sup>a</sup>	Lovley and Philips, 1987
		Sediment	1200 to 1800	16.8 to 22.1	Current study
Sulfur reduction	S <sup>0</sup>	<i>Desulfuromonas michiganensis</i>	250	2.73	Current study
Methanogenesis	CO <sub>2</sub>	Sediment	N/A	5.2 ± 0.8 <sup>a</sup>	Lovley and Philips, 1987
		Sediment	900 to 2700	5.6 to 37.7	Current study

study conducted by He and Sanford (2004), unlabelled acetate was added to pure cultures and depleted until a threshold was reached. However, the concentration of unlabelled acetate was not measured. Subsequently, [ $^{14}\text{C}$ ]-labeled acetate was added and depleted and the activity of [ $^{14}\text{C}$ ]-acetate remaining was used to calculate the acetate threshold (Sanford, personal communication). However, this value did not account for the unlabelled acetate remaining prior to the addition of [ $^{14}\text{C}$ ]-acetate. Therefore, the thresholds reported in their study may have been greatly underestimated.

Finally, the initial acetate substrate concentrations varied substantially in the different experiments, and it is possible that the initial substrate concentration affects the magnitude of the threshold concentration. In particular, in the present study, the acetate threshold decreased from 111  $\mu\text{M}$  in Fe(III)-reducing batch reactors that were initially supplied with 2.5 mM acetate to 4.8  $\mu\text{M}$  in reactors to which 0.5 mM acetate was initially added. This trend has been observed by others. For example, in an earlier study (Hopkins et al., 1995; Warikoo et al., 1996), the initial concentration of benzoate supplied to syntrophic benzoate-degrading organism was shown to influence the benzoate threshold. As the initial benzoate concentration increased the benzoate threshold also increased. The authors concluded that relationship between the initial and threshold benzoate concentration was linked to thermodynamics. Increased initial benzoate concentrations increased the amount of acetate produced, which decreased the amount of residual  $\Delta\text{G}$  and, thus, increased the threshold benzoate concentration.

#### 4.2.2 Result Obtained from Microcosm Study

The relationship between initial and threshold acetate concentrations was further evaluated using duplicate microcosms constructed with anaerobic sediment and groundwater, as described by Davis (2006). Acetate was initially added to microcosms at approximately 4 mM and resupplied five times at concentration ranging from approximately 0.9 to 2.7 mM whenever the acetate removal reached a plateau or threshold (Figure 4.9). The first five additions of acetate stimulated increases in methane production, suggesting that methanogenesis was the dominant TEAP in the microcosms and that aceticlastic methanogens were active. The acetate thresholds ranged from 5.6 to 37.7  $\mu\text{M}$  (Table 4.6).

Sulfate was added along with the sixth amendment of acetate on day 208 in an attempt to shift the TEAP to sulfate reduction and thereby to evaluate the effect of the dominant TEAP on acetate thresholds. However, the well-established methanogenic community prevented growth of sulfate reducers, as evidenced by a continuous increase in methane accumulation and relatively small change in the sulfate concentration between days 208 and 248. Therefore, the acetate threshold measured during this period (5.8  $\mu\text{M}$ , Table 4.6) probably was controlled by methanogenesis. To further promote a shift in the dominant TEAP to sulfate reduction, the methanogenic inhibitor BES was added to the microcosms along with sulfate and acetate on days 312 and 390. Acetate was subsequently depleted, and the relatively stable methane levels and concomitant decrease in sulfate concentrations in the microcosms suggested that the addition of sulfate and BES did successfully promote

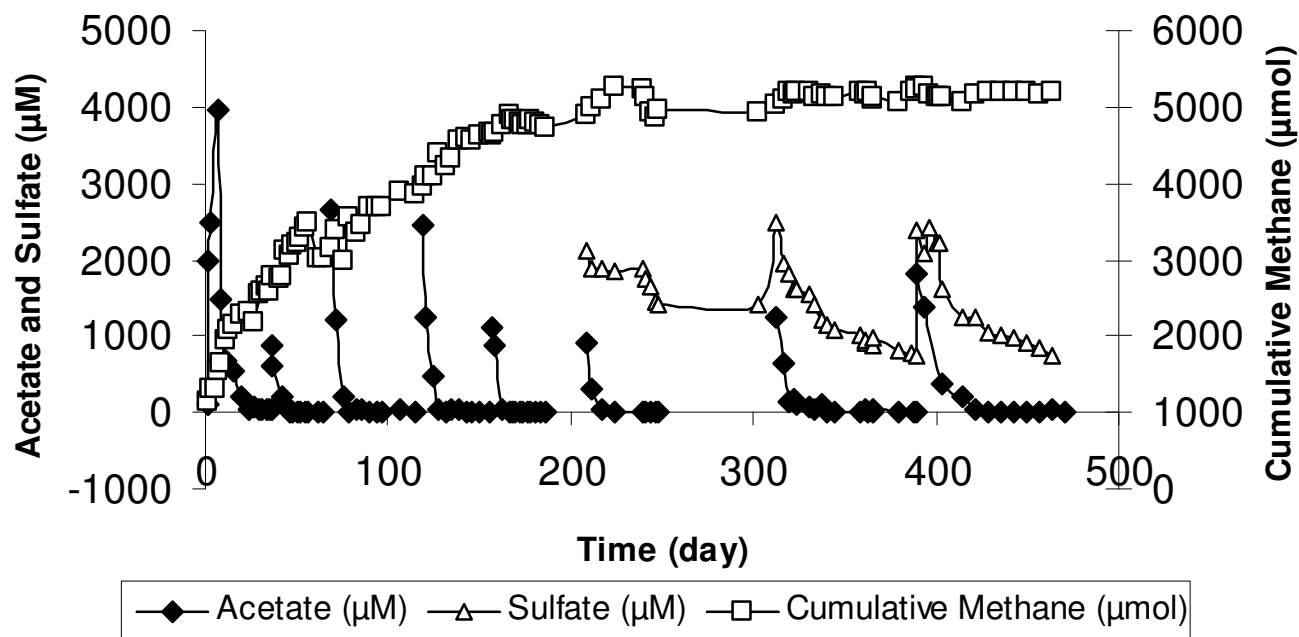


Figure 4.9 Acetate concentrations and cumulative methane production in duplicate microcosms spiked repeatedly with acetate (on days 24, 46, 79, 128, 166, 208, 312, and 390). Sulfate (2 mM) was also added on days 208, 312, and 390. The methanogenic inhibitor BES (2 mM) was also added on days 312 and 390 to promote sulfate reduction. ↓ indicates the first time when sulfate was amended to the reactor.

sulfate-reduction as a dominant TEAP, although some methane production was also observed indicating that methanogenesis was not completely inhibited. The acetate thresholds measured under the mixed sulfate-reducing/methanogenic conditions were 16.8  $\mu\text{M}$  and 22.1  $\mu\text{M}$  (Table 4.6). According to the model of a strictly thermodynamic control on threshold concentrations, thresholds should be lower under sulfate-reducing conditions, which is more thermodynamically favorable, compared with methanogenesis. As summarized in Table 4.6, this trend was not observed in the microcosm reactors. Threshold concentrations measured under sulfate-reducing/methanogenic conditions were similar to, or higher than, the values obtained under strictly methanogenic conditions, particularly when thresholds obtained after the additions of similar initial acetate concentrations are compared.

Table 4.6. Initial and threshold acetate concentrations in duplicate methanogenic sediment microcosms.

Acetate addition <sup>a</sup>	Days corresponding to metabolism of acetate addition	Initial acetate concentration ( $\mu\text{M}$ )	Average acetate concentration ( $\mu\text{M}$ ) <sup>b</sup>
1	24-36	3950	37.7 (16.4)
2	46-65	890	10.5 (4.1)
3	79-97	2670	21.4 (9.0)
4	128-143	2450	26.0 (7.6)
5	166-174	1110	5.6 (0.9)
6 <sup>c</sup>	208-248	911	5.8 (1.9)
7 <sup>c,d</sup>	312-366	1250	16.2 (8.6)
8 <sup>c,d</sup>	390-471	1820	22.1 (8.7)

<sup>a</sup> Acetate additions were made on days 24, 46, 79, 128, 166, 208, 312, and 390, as shown in Figure 4.9.

<sup>b</sup> Values in parenthesis represent  $\pm 1$  standard deviation about average concentration in duplicate microcosms.

<sup>c</sup> Sulfate ( $\sim 2$  mM) added along with acetate.

<sup>d</sup> The methanogenic inhibitor BES was added along with sulfate to promote sulfate reduction.



The difference between experimental results and the reported thresholds and the lack in correlation between the thermodynamic rule and acetate thresholds obtained from both pure culture study and microcosm study could therefore be attributed to the differences in the initial acetate concentrations and the kinetics of electron donor utilization by the active microbes.

The lowest acetate thresholds (measured during the metabolism of the 5th and 6th acetate additions were similar to that previously reported for methanogenic sediment (Table 4.4; Lovley and Phillips, 1987). The thresholds measured during the metabolism of other acetate additions were higher but within the range of acetate thresholds reported for pure cultures of methanogens (Westermann et al., 1989; Min and Zinder, 1989).

Also, it should be noted that thresholds obtained from the laboratory studies and the field studies for a given TEAP should not be compared, because generally the microbes have the ability to use a given substrates found in a mixture at a much lower concentration than when the substrate is provided as a sole C source at high concentration (Kovárová-Kovar and Egli, 1998).

The threshold concentrations in the microcosms measured after each acetate addition were plotted as a function of the initial acetate concentrations in Fig 4.10. A linear regression through the data suggests that the initial and threshold acetate concentrations are correlated. As previously mentioned, thermodynamic factors have previously been used to explain a correlation between initial and threshold acetate

concentrations (Hopkins et al., 1995; Warikoo et al., 1996; Min and Zinder, 1989). Although, thermodynamics did not appear to play an important role in the pure culture studies described above, it is possible that thermodynamic factors may have influenced the acetate thresholds measured in the microcosms. However, acetate thresholds measured in the microcosm reactors should not be influenced by thermodynamic factor alone. As pointed out by Min and Zinder (1989), if the acetate thresholds were solely controlled by thermodynamics, the accumulation of metabolic byproducts, occurring after multiple additions of acetate, would have increased the acetate thresholds greatly. Thus, it is possible that there are other factors controlling thresholds in mixed cultures, and these factors are different than those at play in the pure cultures. Therefore, additional work is needed to explain the apparent relationship between the initial and threshold acetate concentrations in the pure culture and microcosm studies.

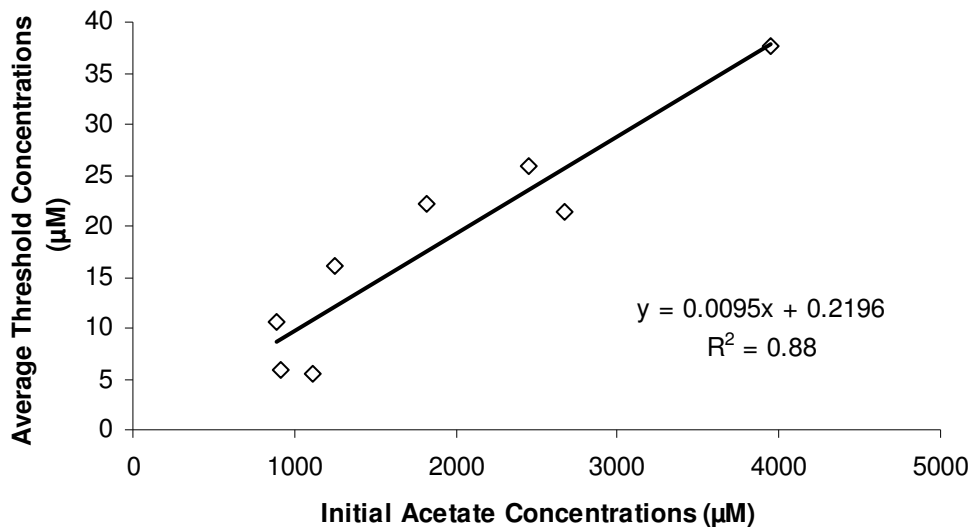


Figure 4.10. Acetate thresholds as a function of initial acetate concentrations in duplicate sediment microcosms under methanogenic and sulfate-reducing conditions. Each data point represents the average concentrations in duplicate microcosms.

## Chapter 5

### Conclusion and Recommendations for Future Work

The overall goal of this research project was to improve our understanding of the relationship between the dominant TEAP and acetate thresholds and evaluate the usefulness of acetate thresholds as an indicator of biodegradation in contaminated subsurfaces.

To achieve this goal, an integrated experimental study of two pure cultures and environmental samples and modeling evaluations were conducted. The threshold experimental results demonstrated that characteristic thresholds existed but did not followed thermodynamic rules as reported in previous studies. The lowest acetate threshold measured with *Geobacter metallireducens* (strain GS-15) was found under Fe(III)-reducing conditions, which yields less free energy compared to Mn(IV)- and  $\text{NO}_3^-$ -reducing conditions. Similar results were obtained from threshold experiments involving *Desulfuromonas michiganensis* (strain BB1) under PCE-dechlorinating and  $\text{S}^0$ - and Fe(III)-reducing conditions. Despite the fact that PCE dechlorination does not yield the greatest amount of free energy among the three TEAPs evaluated, the lowest acetate threshold was observed under PCE-dechlorinating conditions.

A model of microbial respiration was used to further evaluate the potential role of thermodynamics as well as kinetic factors in controlling the acetate thresholds in the pure cultures. The kinetic terms in the model were fit to substrate depletion data collected under electron donor- and electron acceptor-limiting conditions and were

tested using substrate depletion data collected under dual substrate-limiting conditions. The model evaluations indicated that the thermodynamic driving force for acetate metabolism remained high when acetate metabolism ceased and thus confirmed that thermodynamics did not play an important role in controlling the acetate thresholds. However, the model evaluations suggested that the acetate thresholds in both strains were influenced by the kinetics of electron donor utilization.

In experiments conducted with anaerobic microcosms containing sediment and groundwater the acetate thresholds measured under  $\text{SO}_4^{2-}$ -reducing and methanogenic conditions did not appear to be characteristic of the dominant TEAP, although it is likely that multiple TEAPs were occurring concomitantly, particularly under  $\text{SO}_4^{2-}$ -reducing conditions. However, the experimental results strongly suggested that acetate thresholds were correlated with the initial acetate concentrations in the microcosms. These results could suggest that thermodynamics may play a key role in controlling the acetate thresholds in the heterogeneous environmental samples.

In conclusion, the results of this study improve our understanding of the factors affecting acetate thresholds under different conditions, and this knowledge can potentially be useful in interpreting data obtained from sites with on-going bioremediation. However, additional work is needed to investigate the relationship between the initial and threshold acetate concentrations in the pure culture and microcosm studies. Further investigation of the metabolic pathways of acetotrophs capable of using each TEAP will also improve our ability to model acetate utilization using the microbial respiration model and thus refine our understanding of the roles

that kinetics and thermodynamics play in controlling acetate thresholds under a given TEAP.

## References

- Alberty, R. A.** 1998. Calculation of standard transformed Gibbs energies and standard transformed enthalpies of biochemical reactants. *Arch. Biochem. Biophys.* **353**:116-130.
- Barcelona, M. J., D. Tomczak, J. Lu, and C. Virkhaus.** 1993. Fractionation and identification of organic matter in natural and fossil-fuel contaminated aquifer systems, p. 163-176. Proceedings of the API-NGWA 1993 Petroleum Hydrocarbons and Organic Chemicals in Ground Water: Prevention, Detection, and Restoration, Houston.
- Bradford, M.** 1976. A rapid and sensitive method for the quantification of microgram quantities of protein utilizing the principle of protein-dye binding. *Anal. Biochem.* **72**:248-254.
- Brown, E., M. W. Skougstad, and M. J. Fishman.** 1970. Methods for collection and analysis of water samples for dissolved minerals and gases. Techniques of Water Resources Investigations of the U.S. Geol. Survey, U.S. Govt. Printing office, Washington, D. C.
- Bauchop, T., and S. R. Elden.** 1960. The growth of microorganisms in relation to their energy supply. *J. Gen. Microbiol.* **23**:457-469.
- Champine, J. E., B. Underhill, J. M. Johnson, W. W. Lilly, and S. Goodwin.** 2000. Electron transfer in the dissimilatory iron-reducing bacterium *Geobacter metallireducens*. *Anaerobe.* **6**:187-196.
- Chapelle, F. H., S. K., Haack, P. Adriaens, M. A. Henry and P. M. Bradley.** 1996. Comparison of E(h) and H<sub>2</sub> measurements for delineating redox processes in a contaminated aquifer. *Environ. Sci. Tech.* **30**:3565-3569.
- Chapelle, F. H., D. A. Vroblesky, J. C. Woodward, and D. R. Lovley.** 1997. Practical consideration for measuring hydrogen concentrations in groundwater. *Environ. Sci. Tech.* **31**:2873-2877.
- Chapelle, F. H., and D. R. Lovley.** 1992. Competitive-exclusion of H<sub>2</sub> sulfate reduction by Fe(III)-reducing bacteria – a mechanism for producing discrete zones of high iron groundwater. *Ground Water.* **30**:29-36.
- Chapelle, F. H., P. M. Bradley, D. R. Lovley, K. O'Neill, and J. E. Lanmeyer.** 2002. Rapid evolution of redox processes in a petroleum hydrocarbon-contaminated aquifer. *Water.* **40**:353-360.

- Cookson, J. T.** 1995. Bioremediation engineering design and application. McGraw-Hill, Inc., New York.
- Cord-Ruwisch, R., H. Seitz, and R. Conrad.** 1988. The capacity of hydrogenotrophic anaerobic bacteria to compete for traces of hydrogen depends on the redox potential of the terminal electron acceptor. *Arch. Microbiol.* **149**:350-357.
- Cozzarelli, I. M. , M. J. Baedecker, J. M. Fischer and C. S. Phinney.** 1994. Groundwater contamination by petroleum-hydrocarbons-natural biodegradation in a dynamic hydrologic and geochemical system. Abstract of Papers of the American Chemical Society. 208:80-ENVR.
- Davis, G. E.** 2006. Effect of terminal electron accepting processes on acetate thresholds in contaminated sediments. Master Thesis Research. Civil and Environmental Engineering Dept. University of Maryland, College Park.
- Ferguson, T. J. and R. A. Mah.** 1983. Isolation and characterization of an H<sub>2</sub>-oxidizing thermophilic methanogen. *Appl. Environ. Microbiol.* **45**:265-274.
- Freedman, D. L., and J. M. Gossett.** 1991. Biodegradation of dichloromethane and its utilization as a growth substrate under methanogenic conditions. *Appl. Environ. Microbiol.* **57**:2847-2857.
- Gossett, J. M.** 1985. Anaerobic degradation of C<sub>1</sub> and C<sub>2</sub> chlorinated hydrocarbons. NTIS no. AD-A165 055/0. Engineering & Services Laboratory, U. S. Air Force Engineering and Services Center: Tyndall Air Force Base, FL.
- Gossett, J. M.** 1987. Measurement of Henry's law constants for C<sub>1</sub> and C<sub>2</sub> chlorinated hydrocarbons. *Environ. Sci. Technol.* **21**:202-208.
- Grady, C. P. L., B. F. Smets, and D. S. Barbeau.** 1996. Variability in kinetic parameter estimates: a review of possible causes and a proposed terminology. *Wat. Res.* **30**:742-748.
- Hägglom, M. M., and I. D. Bossert** (ed.). 2003. Dehalogenation microbial processes and environmental applications. Kluwer Academic Publishers, Boston U.S.A.
- He, Q. and R. A. Sanford.** 2004. Acetate threshold concentrations suggest varying energy requirements during anaerobic respiration by *Anaeromyxobacter dehalogenans*. *Appl. Environ. Microbiol.* **70**:6940-6943.
- Heimann, A. C., and R. Jakobsen.** 2006. Experimental evidence for a lack of thermodynamic control on hydrogen concentrations during anaerobic degradation of chlorinated ethenes. *Environ. Sci. Technol.* **40**:3501-3507.

- Hopkins, B. T., M. J. McInerney, and V. Warikoo.** 1995. Evidence of an anaerobic syntrophic benzoate degradation threshold and isolation of the syntrophic benzoate degrader. *Appl. Environ. Microbiol.* **61**:526-530.
- Hoehler, T. M., M. J. Alperin, D. B. Albert, and C. S. Martens.** 1998. Thermodynamic control on hydrogen concentrations in anoxic sediment. *Geochim. Cosmochim. Acta.* **62**:1745-1756.
- Huang, D.** 2007. University of Maryland, College Park, MD. Personal Communication.
- Hutson, S. S., N. L. Barber, J. F. Kenny, K. S., Linsey, D. S. Lumia, and M. A., Maupin.** 2004. Estimated use of water in the United States in 2000. U.S. Geological Survey Circular 1268.
- Jin, Q., and C. M. Bethke.** 2002. Kinetics of electron transfer through the respiratory chain. *Biophysical J.* **83**:1797-1808.
- Jin, Q., and C. M. Bethke.** 2003. A new rate law describing microbial respiration. *Appl. Environ. Microbiol.* **69**:2340-2348.
- Jin, Q., and C. M. Bethke.** 2005. Predicting the rate of microbial respiration in geochemical environments. *Geochimica et Cosmochimica Acta.* **69**:1133-1143.
- King, G. M.** 1991. Measurement of acetate concentrations in marine pore waters by using an enzymatic approach. *Appl. Environ. Microbiol.* **57**:3476-3481.
- Kovárová-Kovar, K., and T. Egli.** 1998. Growth kinetics of suspended microbial cells: From single-substrate-controlled growth to mixed-substrate kinetics. *Microbiol. Mol. Biol. Rev.* **62**:646-666.
- Krumholz, L. R.** 1997. *Desulfuromonas chloroethenica* sp. nov. uses tetrachloroethylene and trichloroethylene as electron acceptors. *International J. of Systematic Bacteriology.* **47**:1262-1263.
- Liu C., Y. A. Gorby, J. M. Zachara, J. K. Fredrickson, C. E. Brown.** 2002. Reduction kinetics of Fe(III), Co(III), U(VI), Cr(VI), and Tc(VII) in cultures of dissimilatory metal-reducing bacteria. *Biotechnology & Bioengineering.* **80**: 637-649.
- Löffler, F. E., R. A. Sanford, and J. M. Tiedje.** 1996. Initial characterization of a reductive dehalogenase from *Desulfitobacterium chlororespirans* Co23. *Appl. Environ. Microbiol.* **62**:3809-3813.
- Löffler, F. E., J. M. Tiedje, and R. A. Sanford.** 1999. Fraction of electrons consumed in electron acceptor reduction and hydrogen thresholds as indicators of halorespiratory physiology. *Appl. Environ. Microbiol.* **65**:4049-4056.



- Lovley, D. R.** 2007. University of Massachusetts, Amherst, MA. Personal Communication.
- Lovley, D. R. and E. J. Phillips.** 1987. Competitive mechanisms for inhibition of sulfate reduction and methane production in the zone of ferric iron reduction in sediments. *Appl. Environ. Microbiol.* **53**:2636-2641.
- Lovley, D. R., and E. J. Phillips.** 1988a. Novel mode of microbial energy metabolism: organic carbon oxidation coupled to dissimilatory reduction of iron and manganese. *Appl. Environ. Microbiol.* **54**(6): 1472-1480.
- Lovley, D. R., and S. Goodwin.** 1988b. Hydrogen concentrations as an indicator of the predominant terminal electron accepting reactions in the aquatic sediments. *Geochimica. et. Cosmochimica Acta.* **52**:2993-3003.
- Lovley, D. R., F. H. Chapelle, and J. C. Woodward.** 1994. Use of Dissolved H<sub>2</sub> Concentrations to Determine Distribution of Microbially Catalyzed Redox Reactions in Anoxic Groundwater. *Environ. Sci. Technol.* **28**:1205-1210.
- McCarty, P. L.** 1972. Energetics of organic matter degradation, p. 91-118. In R. Mitchell (ed.), *Water pollution Microbiology*, vol. 1. Wiley-Interscience, New York.
- McMahon, P. B., and F. H. Chapelle.** 1991. Microbial production of organic acids in aquitard sediments and its role in aquifer geochemistry. *Nature.* **349**:233-235.
- Min, H. and S. H. Zinder.** 1989. Kinetics of acetate utilization by two thermophillic acetotrophic methanogens: *Methanosarcina* sp. Strain CALS-1 and *Methanotherix* sp. Strain CALS-1. *Appl. Environ. Microbiol.* **55**:488-491.
- NRC.** 2000. Natural attenuation for groundwater remediation. National Research Council. National Academy Press, Washington D.C.
- Russell, J. B., and M. C. Gregory.** 1995. Energetics of bacterial growth: balance of anabolic and catabolic reactions. *Microbiol. Rev.* **59**:48-62.
- Rittmann, B. E.** 1987. Aerobic biological treatment. *Environ. Sci. Tech.* **21**:128-136.
- Rittmann, B. E., E. Seagren, B. A. Wrenn, A. J. Valocchi, C. Ray, and L. Raskin.** 1994. *In Situ Bioremediation.* 2<sup>nd</sup> ed. Noyes Publications, Park Ridge, NJ.
- Rittmann, B. E., and P. L. McCarty.** 2001. *Environmental Biotechnology: Principles and Applications.* The McGraw-Hill Companies, New York.
- Seagren, E. A., and J. G. Becker.** 1999. Organic acids as a bioremediation monitoring tool, P. 343-348. In B. C. Allenman and A. Leeson (ed.), *Natural*

attenuation of chlorinated solvents, petroleum hydrocarbon, and other organic compounds. Battelle Press, Columbus, OH.

**Seagren, E. A., and J. G. Becker.** 2002. Review of natural attenuation of BTEX and MTBE in groundwater. Practice Periodical of Hazardous, Toxic, and Radioactive Waste Management, ASAE. 6:156-172.

**Senko, J. M., and J. F. Stolz.** 2001. Evidence for iron-dependent nitrate respiration in the dissimilatory iron-reducing bacterium *Geobacter metallireducens*. Appl. Environ. Microbiol. **65**:3750-3752.

**Snoeyink, V. L., and D. Jenkins.** 1980. Water Chemistry. John Wiley & Sons, Inc., New York.

**Sommer, H. M., H. Spliid, H. Holst, and E. Arvin.** 1998. Examination of reproducibility in microbiological degradation experiments. Biodegradation. **9**:65-82.

**Squillace, P. J., J. M. Michael, and C. V. Price.** 2004. VOCs in shallow groundwater in new residential/commercial areas in the United States. Environ. Sci. Tech. **38**:5327-5338.

**Stumm, W., and J. J. Morgan.** 1996. Aquatic Chemistry. John Wiley & Sons, Inc., New York.

**Sung, Y., K. M. Ritalahti, R. A. Sanford, J. W. Urbance, S. J. Flynn, J. M. Tiedje, and F. E. Löffler.** 2003. Characterization of two tetrachloroethene-reducing, acetate-oxidizing anaerobic bacteria and their description as *Desulfuromonas michiganensis* sp. nov. Appl. Environ. Microbiol. **69**:2964-2974.

**Sung, Y., K. F. Fletcher, K. M. Ritalaliti, R. P. Apkarian, N. Ramos-Hernandez, R. A. Sandford, N. M. Mesban, and F. E. Löffler.** 2006. *Geobacter lovleyi* sp nov strain SZ, a novel metal-reducing and tetrachloroethene-dechlorinating bacterium. Appl. Environ. Microbiol. **72**:2775-2782.

**Su, X.** 2004. Evaluation of acetate thresholds under various terminal electron-accepting conditions: application to bioremediation monitoring. Master Thesis Research. Biological Resources Engineering Dept. University of Maryland, College Park.

**Thauer, R. K., D. Möller-Zinkhan, and A. M. Spormann.** 1989 Biochemistry of acetate catabolism in anaerobic chemotrophic bacteria. Ann. Rev. Microbiol. **43**:43-67.

**Thauer, R. K., K. Jungermann, and K. Decker.** 1997. Energy conservation in chemotrophic anaerobic bacteria. Bacteriol. Rev. **41**:100-179.

**Vroblesky, D. A., P. M. Bradley, and F. H. Chapelle.** 1997. Lack of correlation between organic acid concentrations and predominant electron-accepting processes in a contaminated aquifer. Environ. Sci. Tech. **31**:1416-1418.

**Warikoo, V., M. J. McInerney, J. A. Robinson, and J. M. Suflita.** 1996. Interspecies acetate transfer influences the extent of anaerobic benzoate degradation by syntrophic consortia. *Appl. Environ. Microbiol.* **62**:26-32.

**Watson, I. A., S. E. Oswald, K. U. Mayer, Y. Wu, and S. A. Banwart.** 2003. Modeling kinetic processes controlling hydrogen and acetate concentrations in an aquifer-derived microcosm. *Environ. Sci. Tech.* **37**:3910-3919.

**Westermann, P., B. K. Ahring, R. A. Mah.** 1989. Acetate production by methanogenic bacteria. *Appl. Environ. Microbiol.* **55**:2257-2261.

**White, D.** 1995. *The physiology and biochemistry of prokaryotes.* Oxford University Press, Inc., New York.